Phage-host interactions and the dynamic nature of tRNA modification during the infection cycle of a tailed bacteriophage and cold-active bacterium from Baltic Sea ice

Niklas Ahlblad

2021

Master's Thesis

University of Helsinki
Faculty of Biological and Environmental Sciences
Master's Programme in Genetics and Molecular Biosciences

Tiedekunta – Fakultet – Faculty	Koulutusohjelma – Utbildingsprogram – Degree Programme
Faculty of Biological and Environmental Sciences	Master's Programme in Genetics and Molecular Biosciences

Tekijä – Författare – Author
Niklas Christoffer Viktor Ahlblad

Työn nimi – Arbetets titel – Title
Phage-host interactions and the dynamic nature of tRNA modification during the infection cycle of a tailed bacteriophage and cold-active bacterium from Baltic Sea ice

Oppiaine/Opintosuunta – Läroämne/Studieinriktning – Subject/Study track
Biochemistry and Structural Biology

Työn laji – Arbetets art – Level	Aika – Datum – Month and year	Sivumäärä – Sidoantal – Number of pages
Master's thesis	07.2021	49

Tiivistelmä – Referat – Abstract

The infection mechanisms between cold-active bacteria and their respective bacteriophages are currently relatively unknown and undocumented. *Shewanella* sp. 4 is a cold-active bacterium that was recently isolated from Baltic Sea ice along with bacteriophage isolate 1/4. Little is known about this particular isolate, although many *Shewanella* species have important environmental roles incl. carbon cycling, and they have also been associated with the spoilage of fishery products and bioremediation.

Previous studies have shown that an infection caused by bacteriophages may lead to significant changes in transfer RNA (tRNA) modifications in the host cell. Commonly, tRNA modification levels may be altered as a response to different stressors, to which viral infections belong as well. Bacteriophages may take advantage of tRNA modifications during the infection of their host, as changes in tRNA modifications lead to much faster response than affecting only the transcription and translation machineries.

Here, the infection cycle and changes in tRNA modifications in *Shewanella* sp. 4 were investigated, along with using a more defined growth media and comparing it to previously conducted characterization. A multitude of methods were applied, such as transmission electron microscopy and mass spectrometry, to observe both the infection mechanisms and changes in tRNA modifications over the course of the infection.

I found that the infection cycle of the phage-host pair is predictable and consistent with previously conducted research, lasting 3 hours until cell lysis. Plaque assay and SDS-PAGE showed the release of virions 2-3 h post-infection (p.i.), and the production of viral proteins within cells starting from 100 min p.i. An intriguing periodic change in cell turbidity was also observed already before cell lysis. Furthermore, the tRNA modifications m^1A, m^5U, m^6t^6A, and Cm undergo statistically significant changes or display high variance during the course of the infection when comparing infected and uninfected cells. These may affect tRNA structural stability, translational accuracy, and cleavage in the host cell, showing possible importance during the infection.

Understanding the fundamentals of the infection mechanisms involved in this bacterium-bacteriophage pair gives further insight into their role in the Baltic Sea ecosystem. This is especially relevant for establishing *Shewanella* as a potential laboratory model for studying molecular mechanisms that further cold-active metabolism.

Avainsanat – Nyckelord – Keywords
Baltic Sea, *Shewanella*, Phage 1/4, tRNA modifications

Ohjaaja tai ohjaajat – Handledare – Supervisor or supervisors
Mirka Lampi & Peter Sarin

Säilytyspaikka – Förvaringställe – Where deposited
HELDA

Muita tietoja – Övriga uppgifter – Additional information

Tiedekunta – Fakultet – Faculty	Koulutusohjelma – Utbildingsprogram – Degree Programme
Bio- och miljövetenskapliga fakulteten	Magisterprogrammet i genetik och molekylära biovetenskaper

Tekijä – Författare – Author
Niklas Christoffer Viktor Ahlblad

Työn nimi – Arbetets titel – Title
Fag-värd interaktioner och tRNA modifikationernas dynamiska natur under infektionscykeln av en svansad bakteriofag och en kallaktiv bakterie från Östersjöis

Oppiaine/Opintosuunta – Läroämne/Studieinriktning – Subject/Study track
Biokemi och strukturbiologi

Työn laji – Arbetets art – Level	Aika – Datum – Month and year	Sivumäärä – Sidoantal – Number of pages
Magisteravhandling	07.2021	49

Tiivistelmä – Referat – Abstract

Infektionsmekanismerna mellan kallaktiva bakterier och deras respektive bakteriofager är för tillfället relativt okända och odokumenterade. *Shewanella* sp. 4 är en kallaktiv bakterie som nyligen isolerats tillsammans med bakteriofagisolat 1/4 från ett stycke is från Östersjön. Trots att många *Shewanella*-arter har viktiga miljörelaterade roller och deltar i biogeokemiska kretslopp, som t.ex. kolcykling, samt att de är associerade med förruttning av fiskeriprodukter och bioremediering, så vet vi mycket litet om detta isolat.

Tidigare studier har visat att en infektion förorsakad av bakteriofager kan leda till signifikanta förändringar i transport-RNA (tRNA) modifikationer i värdcellen. Allmänt sett förändras tRNA modifikationernas nivåer som en respons till olika stressfaktorer, till vilket även en virusinfektion hör. Bakteriofager kan utnyttja tRNA modifikationer under infektionen av deras värd, eftersom förändringar i tRNA modifikationer kan leda till en mycket snabbare respons jämfört med en omfattande omprogrammering av transkriptions- och translationsmaskinerierna.

I detta arbete har jag undersökt infektionscykeln och förändringar i tRNA modifikationer hos *Shewanella* sp. 4 samt utforskat användningen av ett definierat tillväxtmedia och jämfört detta med tidigare karakterisering. En mängd olika metoder tillämpades, som till exempel transmissionselektronmikroskopi och masspektrometri, för observation av både infektionsmekanismerna och förändringarna i tRNA modifikationer under infektionens förlopp.

I enlighet med tidigare resultat så fastställde jag att bakteriofag-värdcellens infektionscykel är förutsägbar och konsistent med en varaktighet av 3 timmar tills cellys. Plackanalys och SDS-PAGE visade frilösning av virioner 2-3h post-infektion (p.i.), och produktionen av virusproteiner i celler kan skönjas från och med 100 min p.i. Utöver detta så observerades en intressant periodisk förändring i cellturbiditeten redan före cellys. Dessutom genomgår tRNA modifikationerna m^1A, m^5U, m^6t^6A och Cm statistiskt signifikanta förändringar, eller så uppvisar de en hög varians under infektionens lopp då man jämför infekterade och oinfekterade celler. Dessa modifikationer kan ha en betydande påverkan på tRNA-molekylens strukturella stabilitet, translationsnoggrannheten och tRNA klyvning i värdcellen, vilket kan vara av avsevärd betydelse under infektionsloppet.

En grundläggande förståelse av infektionsmekanismerna i detta bakterie-bakteriofagpar kommer att ge ytterligare insikt till deras roll i Östersjöns ekosystem. Detta är relevant speciellt för att etablera *Shewanella* som en potentiell laboratoriemodell för att undersöka de molekylära mekanismer som möjliggör en kallaktiv metabolism.

Avainsanat – Nyckelord – Keywords
Östersjön, *Shewanella*, Fag 1/4, tRNA modifikationer

Ohjaaja tai ohjaajat – Handledare – Supervisor or supervisors
Mirka Lampi & Peter Sarin

Säilytyspaikka – Förvaringställe – Where deposited
HELDA

Muita tietoja – Övriga uppgifter – Additional information

Table of Contents

1 Abbreviations

rMB – Rich marine broth

MOI – Multiplicity of infection

vtRNA – Virus-encoded tRNA

OD – Optical density

SD – Standard deviation

TCA – Trichloroacetic acid

TBE – Tris-Borate-EDTA

SDS-PAGE – Sodium dodecyl sulphate-polyacrylamide gel electrophoresis

BCP – 1-bromo-3-chloropropane

TEM – Transmission Electron Microscopy

UPLC-MS – Ultra-performance Liquid Chromatography Mass Spectrometry

TIC – Total ion chromatogram

XIC – Extracted ion chromatogram

2 Introduction

Shewanella sp. 4 is a Gram-negative, rod-shaped bacterium found in the land-fast sea ice of the Baltic Sea (Luhtanen et al., 2014). Strain 4 is cold-active, meaning it maintains essential metabolic activity in an environment with low temperatures. *Shewanella* is the only genus of the family *Shewanellacae*, a marine bacterial family. Many of the other members belonging to this family have been isolated and characterized, although strain 4 has remained uncharacterized. However, the characterization of related species of *Shewanella*, namely *S. putrefaciens* and *S. baltica*, points towards strain 4 having a possible role in the spoilage of fishery products and bioremediation (Jørgensen & Huss, 1989; Vogel et al., 2005; Dikow et al., 2011).

Bacteriophage isolate 1/4, which infects strain 4, represents a myovirus morphotype with an icosahedral head and helical tail. Originally, phage 1/4 was isolated from melted sea ice samples through filtration and plaque purification (Luhtanen et al., 2014). In addition to isolating the bacteriophage, Luhtanen and colleagues analysed the genome of the phage, and found that it consists of 235 genes, of which 26 encode structural proteins.

The genome has also been shown to contain two genes encoding tRNA, adding interest to continued research.

The usual lytic infection cycle of a bacteriophage can be divided into a few simplified processes: initial infection, production of viral components using the resources and cellular machineries of the host, assembly of said components into new phages, and lastly, the release of infectious viral particles by either passive or active lysis (Kasman & Porter, 2020). So far, it is understood that bacteriophage isolate 1/4 uses the lytic cycle for its replication, which has been previously observed using low numbers of phages versus host cells in cultures (Senčilo et al., 2015). Additionally, a putative abortive infection has been suggested as an outcome of the infection. An extensively studied event, abortive infections lead to cellular “suicide” before the next generation of phages have been fully produced, thus protecting other cells from infection (Molineux, 1991). This altruistic mechanism can still be avoided by the invading phage through mutations or the production of antitoxins for binding of the bacterial toxin (Samson et al., 2013). This has been previously suggested as an outcome of strain 4 infection by phage 1/4, as the genome annotation has shown genes for a toxin and antitoxin, namely from systems RelE/ParE toxin and RelB/DinJ antitoxin families (Qasim, unpublished data).

Generally, bacteriophages play an important role in the balance of the sea ecosystem by limiting bacterial population growth and regulating the community compositions (Weitz & Wilhelm, 2012). Approximately 10^{23} viral infections take place in the oceans every second, and 20% of the marine microbial biomass is recycled daily, displaying the significance of bacteriophages in the oceanic cycles (Suttle, 2007). Bacterial mortality following viral infection releases organic carbon and other nutrients back into the environment, thus contributing to the biogeochemical cycle of the sea through this so called “viral shunt” (Wilhelm & Suttle, 1999). Normally, a delicate balance exists between the number of marine bacteriophages and their host bacteria. However, given the variability of the Baltic Sea ecosystem, major differences between microorganism communities and viral infection rates, along with bacterial cell mortality, exist (Holmfeldt et al., 2010). Marine phage-host pairs have been a topic of active research in recent decades, with some of the latest studies focusing on the resistance mechanisms of the host, the characteristics of extremophilic bacteria, and the interactions between novel strains and phages in different oceanic environments (Liu et al., 2006; Wang & Zhang, 2010; Horvath & Barrangou, 2010; Wei & Zhang,

2010; Luhtanen et al., 2014; Luhtanen et al., 2018). However, certain aspects of infection, such as antiviral mechanisms in hosts, remain less studied in marine phage-host pairs than their terrestrial counterparts (Jin et al., 2019). Regardless, given the unique composition of the Baltic Sea, the phage-host pairs may display different traits compared to other oceanic ecosystems. Moreover, apart from importance in the environment, a fundamental understanding of the strain 4 and the phage 1/4 infection is required in order to establish a possible laboratory model utilizing this host-phage pair.

2.1 Mechanisms of infection and host response

The primary means of influencing a hosts' physiology during infection happens through changes in the transcriptional and translational machineries. As bacteriophages, and viruses in general, lack their own translational mechanism, they must instead take advantage of the host to translate viral messenger-RNAs (mRNAs) and produce proteins essential for replication. This is made possible by recruitment and take-over of the hosts' well-organized and controlled transcription, translation factors, and signalling pathways, while avoiding defence responses. The virus has some options when it comes to seizing control over the hosts' transcription: outcompete the normal transcription of host genes and direct it towards the viral genome, or target host mRNA directly (Rohrmann, 2019). In addition, viruses may encode their own transcriptional activators and enhancers, which aid the virus in assembling host cell transcription complexes for RNA initiation of viral genes instead of host genes. Moreover, some viruses target specific host factors, such as ribosomal proteins (RPs), and cleave important host proteins, to alter the translational machinery in favour of the virus (Walsh et al., 2013; Li, 2019). The efficiency of viral mRNA translation is further promoted by the impairment of host mRNA translation. Other viruses rely on seizing control of the host ribosomes by utilizing an untranslated region of viral mRNA, called viral internal ribosome entry sites (IRES), for initiation of viral protein synthesis (Bushell & Sarnow, 2002). Furthermore, a common strategy is to target the mRNA metabolism of the host to reduce the efficiency of host mRNA translation and stability, instead stabilizing phage transcripts for phage protein production (Marchand et al., 2001; Walsh et al., 2013; Dendooven et al., 2017).

Avoidance of host cell defence response is also a crucial part of the survivability of the virus. Physical barriers in the form of factors such as receptor regulation, extracellular polymeric substances (EPSs), and superinfection exclusion (Sie), present the first defence

against phage adsorption and subsequent viral genome injection (Breitbart, 2012; Labrie et al., 2010; Dy et al., 2014). If a bacteriophage successfully avoids these, a subsequent invasion of the host cell induces further cellular responses to neutralize the threat posed by the phage. For example, the innate bacterial immune response of restriction-modification systems is utilized in this case to protect the host cell by prevention of phage proliferation (Vasu & Nagaraja, 2013). However, bacteriophages have evolved, and continue to evolve, their own equipment to combat these defence mechanisms, such as degradation of extracellular components, leading to a constant arms race between phage and host (Hanlon et al., 2001; Hampton et al., 2020). After successful infection despite host cell defences, viral proteins are produced as a result of viral genome translation, leading to a variety of stress responses. For example, responses such as SOS response and heat shock regulon have been found in *Salmonella enterica* and *Escherichia coli* as a result of bacteriophage infection (Campoy et al., 2006; Osterhout et al., 2007).

2.2 RNA modifications

Apart from the take-over of host cell machinery, attention has been heavily directed towards the possible role of RNA modifications in viral infections. A variety of RNA modifications are present in a large number of species, indicating evolutionary conservation (Schaefer et al., 2017). Additionally, modifications can occur in every type of RNA. Each nucleoside in an RNA molecule can be modified, leading to non-reliance on sequence information as the sole template for functionality (Schaefer et al., 2017). These chemical modifications can include for example methylation, adenylation, isomerization, or hydroxylation (Roundtree et al., 2017; Sakai et al., 2019). Modifications can as well be more complex and require complicated modification pathways (Boo & Kim, 2020). One of the most common modifications, Nm (2'-O-methylation), has a variable function depending on its' localization, although it is mostly associated with tRNA stability and translational accuracy (Dimitrova et al., 2019). Enzymes, such as methyltransferases (MTases) in the case of Nm, regulate the post-transcriptional modification of RNAs, leading to the formation of unique chemical and structural properties for each moiety (Netzband & Pager, 2020). To date, over 150 unique RNA modifications have been characterized on all four canonical ribonucleotides, along with non-canonical nucleotides such as pseudouridine (Ψ) (Boccaletto et al., 2018). In recent years, thanks to technological advancements, these modifications have been confirmed to exist in

all RNAs. In addition to increasing interest, the recently developed and improved methods, such as next-generation sequencing (NGS) and mass spectrometry, have significantly promoted ongoing research regarding the previously unknown functions and purpose of RNA modifications (Schaefer et al., 2017).

2.3 Role of tRNA modifications

Transfer-RNA (tRNA) is an essential molecule in translation for all forms of life, serving as a bridge between the genetic code and functional proteins. Regardless of having such a central role in translation for all organisms, the specifics of interaction between tRNA, mRNA, and ribosomes are still poorly understood (Koh & Sarin, 2018). Out of the known RNA-molecules, tRNA also carries the highest density of post-transcriptional modifications (Lorenz, Lünse & Mörl, 2017). These modifications broaden the capabilities of tRNA-molecules by affecting stability, structure, and functions, resulting in improved translational accuracy, protection from restriction, and cell viability (Edwards et al., 2020). Additionally, modifications to specific parts of the tRNA molecule will affect the binding to other factors, such as by providing stability for ribosome-mediated codon binding and promote correct folding to modulate tRNA-mRNA anticodon-codon interactions (Vendeix et al., 2008; Lyons et al., 2018)

These nucleoside modifications are evolutionarily conserved and often serve as an organisms' rapid adaptation to environmental or cellular changes (Koh & Sarin, 2018) (Fig. 1). Such changes include physiological stressors, such as temperature, oxidative stress, high salinity, changes in pH, lack of nutrients, and high cell density, adaptation to which requires a quick response in the organism. Some tRNA modifications only display changes in the event of stress, and do not show importance during normal bacterial growth. Cellular stress response can be controlled, for example, by specific post-transcriptional modifications on tRNA that contribute to codon-bias flexibility for selective translation of mRNAs encoding stress response proteins (Dedon & Begley, 2014). Modifications at or close-by to the anticodon loop of tRNA result in some of the most important changes, as these control fidelity of translation (Endres et al., 2015; Ranjan & Rodnina, 2016). A particularly active area for modification is at the wobble position 34, where a large number of modifications take place, affecting the codon-anticodon interactions of the tRNA molecule (Koh & Sarin, 2018) (Fig. 1). During decoding of the mRNA, the first and second bases of the codon pair

with the positions 35 and 36 of the tRNA anticodon according to Watson-Crick base pairing (Crick, 1966; Suzuki, 2021). The third mRNA codon base binds to the nucleotide in position 34, which does not necessarily follow similar base pairing, instead allowing “wobble pairing”. Modifications to this location may dictate how the codon is read. For example, adenosine at this position can be modified to inosine, which has the ability to pair with adenine, uridine, and cytosine (Agris et al., 2007). This wobble enables rapid translation of genes with codon usage differing from other transcripts, such as stress-related genes. Given the large variety of modifications occurring at this site, position 34 has been suggested to participate in an equally significant number of cellular mechanisms (Rozov et al., 2016).

Furthermore, some bacteriophages carry their own, less studied, virus-encoded tRNAs (vtRNAs) that are thought to modulate translation by providing codons that are uncommon in the target host cell (Cliffe et al., 2008; Dreher, 2010). So far, the expression of two vtRNA genes in phage isolate 1/4 and the modifications of resulting tRNA molecules remains unknown. However, in addition to being prevalent in all forms of life, tRNA modifications are significant for bacteriophages and viruses in general, as some viral genomes contain tRNA-like structures and some encode for tRNA-modifying enzymes (Dreher, 2009; Dreher, 2010). Because of the nature of bacteriophages, a reasonable possibility for the function of vtRNAs is to aid the infection. The phage may also take advantage of the infection induced stress response and utilize tRNA modifications to affect the translation of stress-specific transcripts.

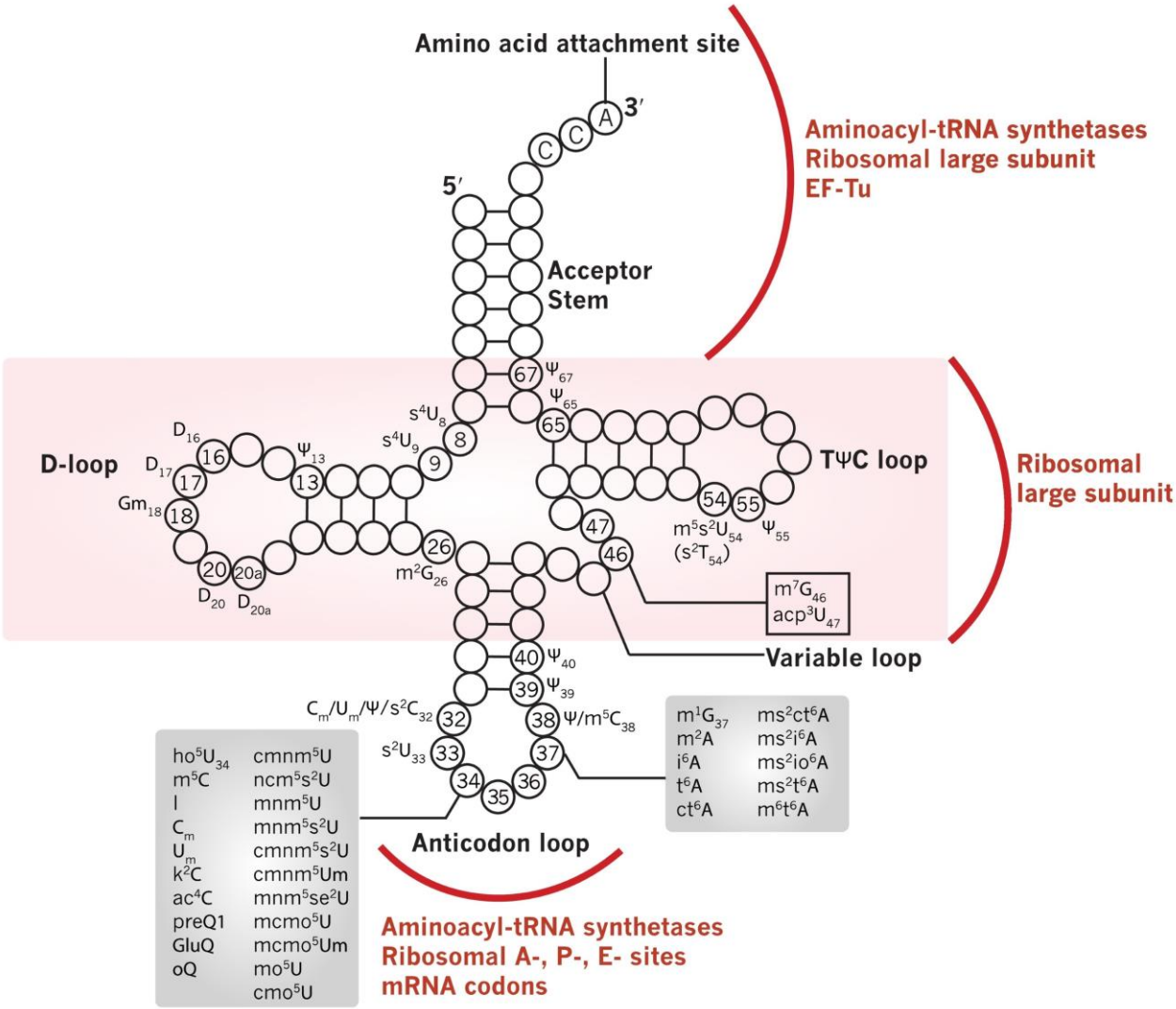

Figure 1: Structure of the tRNA molecule and position and characteristic of post-transcriptional modifications. Domains marked in black. Interaction sites for aminoacyl-tRNA synthetases and ribosomal subunits marked in red. Post-transcriptional modifications highlighted and numbered according to respective positions at which these have been encountered. Figure modified from Koh & Sarin (2018).

2.4 Aims

The aims of this project were firstly to study and understand the infection cycle of the *Shewanella* strain 4-phage 1/4 pair. Different, undefined media and lower number of phages have been used in previous investigations, which is why a thorough examination of the infection cycle was essential. Additionally, the fundamental research is crucial to link any potential tRNA modifications to specific stages of infection and to study the dynamics of the tRNA modificome at different phases. Apart from reaching a fundamental understanding of the infection cycle of the phage-host pair, visualization of the infection allowed for observable

alterations in infected cells to be connected to the infection cycle. Finally, after investigating the infection cycle and visualizing changes in host cells during the infection, a central aim for this project was to connect changes in tRNA modifications found in the host to the infection cycle. Then, the statistically significantly changing tRNA modifications could be connected to specific stages of the infection. The acquired data can subsequently be compared to previously conducted studies regarding the connection between stress response and tRNA modifications to explore potential links, as a viral infection is a significant stressor itself.

3 Materials and methods

3.1 Host bacterium

Bacterial strain used during this project was *Shewanella* sp. 4, previously isolated from Baltic Sea ice (Luhtanen et al., 2014). Strain 4 cells were grown on rich 25% Marine broth (rMB) - agar plates (Supplementary Tables 1 & 2) at +15 °C over 2 nights, after which the plate was stored at +4 °C and used for a maximum of 3 days. Cells originating from previously isolated cultures stored at -80 °C were used to streak fresh plates at equal intervals between each experiment.

For experiments involving liquid cultures, inoculation was conducted from strain 4 colonies on rMB agar plates into 40 ml of rMB, and grown at +15 °C, with 200 rpm aeration over 2 nights. These starter cultures were used to inoculate rMB with enough culture to reach an optical density (OD) value of ~0.2, measured at a wavelength of 600 nm (OD_{600}) with an Eppendorf BioPhotometer D30 (Germany), to be used in further experiments.

3.2 Assessment of the amount of viable cells

The amount of living cells of strain 4 in liquid culture was determined during the early logarithmic growth phase. At this point of growth, the cell division occurs at an increased rate. Inoculation of liquid culture was conducted as described in section 3.1. Growth was then monitored by measuring absorbance at regular intervals. Samples of 1 ml were taken at OD values of 0.5, 0.55, 0.6, 0.65, 0.7 and 0.75. Samples were diluted as dilution series in rMB, and 100 µl of predicted appropriate dilutions were plated and grown at +15 °C over 2 nights. Dilutions of 10^{-4} – 10^{-6} for OD values of 0.5 - 0.6, and 10^{-5} – 10^{-7} for OD values of 0.65 –

0.75 were used. Three replicates of this experiment were conducted, with parallel plates made for each. The OD-values of 0.55, 0.65 and 0.75 were explored once, after which they were not included in the following two repeats. The number of colonies was counted for each plate, based on which the number of cells was calculated. The following formula was used to calculate the number of viable cells in liquid culture.

$$\frac{Number\ of\ colonies}{Dilution\ factor} = Viable\ cell\ count$$

3.3 Bacteriophage

Bacteriophage isolate 1/4 was isolated from the same melted sea ice samples taken from Baltic Sea ice as strain 4 (Luhtanen et al., 2014). A phage agar-stock was provided in the beginning of the project with a titer of 1.9 x 10^{10} pfu/ml (plaque forming units/ml).

3.4 Virus stock production

A pre-existing virus agar stock was used to make a dilution series between concentrations of 10^{-2} – 10^{-11} in rMB. Infection of host cells was conducted by pipetting 100 µl of phage stock dilution, 100 µl of strain 4 culture, and 3 ml of rMB soft agar into test tubes, and plating on rMB agar plates. After growing overnight, the plates were observed to resolve the dilution at which semiconfluency could be seen. Semiconfluency refers to half of the bacterial lawn being lysed. The appropriate dilution for production of semiconfluent plates was shown to be 10^{-4}. Using this dilution, 30 rMB agar plates were prepared, with 3 ml of rMB soft agar added to each. The soft agar layer was scooped into flasks and 2.5 ml rMB was added for each plate, leading to a final volume of ~165 ml. Flasks were subsequently shaken at 15 °C with 200 rpm aeration for 30 min for separation of phages from cell debris and agar. Debris resulting from cell lysis and agar was removed by centrifugation at 7000 *g*, 4 °C for 15 min, after which filtration was conducted to remove any remaining living cells. The filtration was performed twice, using 0.45 µm and 0.2 µm methacrylate-butadiene-styrene (MBS) syringe filters (Sarstedt), after which the resulting phage stock was stored in 4 °C for later use.

3.5 Number of phages in agar stock

The produced phage agar stock was titrated by making serial dilutions of phage in rMB and proceeding as described in section 3.4. The soft agar was tempered to 55 °C to maintain liquid form while avoiding destruction of cells and reduction of phage infectivity due to excessive heat. Resulting plates were incubated in 15 °C over 2 nights, and the formed plaques were counted. Based on the amount of plaques, the amount of infective viral particles was assessed using the following formula.

$$\frac{Number\ of\ plaques}{Dilution\ factor} = Phage\ stock\ titer$$

3.6 Infection of strain 4 by varying number of bacteriophages

The number of phages per host cell is described as the multiplicity of infection (MOI). In this case, the MOI value was altered to see the resulting effect on the infection cycle. MOI values of 0.02, 0.2, 1.0, 2.0, 3.0, 4.0, 6.0, and 10.0 were used in otherwise identical experiments.

Liquid 40 ml and 100 ml cultures of strain 4 were inoculated and grown as described in section 3.1. Two different volumes were used to confirm similarity, as higher culture volumes yield higher amounts of RNA. Culture volumes of 40 ml were used for growth and studying the infection cycle. Larger volumes were used for RNA isolation. The growth was monitored by observing changes in OD_{600} with 1-hour intervals. Once OD_{600} value of 0.6 was reached, and cell growth passed from early log-phase to log-phase, infection with phage agar stock in rMB was conducted. Simultaneously, controls were mock-infected using same volume of rMB. In order to avoid phage adsorption to only a few bacterial cells, the virus stock aliquot applied for infection was mixed with rMB, resulting in a total volume of 2.5 ml for 40 ml cultures, and 5 ml for 100 ml cultures.

The amount of phage stock necessary to reach the desired MOI value was calculated using the following formula.

$$\frac{Viable\ cell\ count\ x\ Volume}{Phage\ stock\ titer} = MOI$$

3.7 Tracking the release of viral particles by plaque assay

Liquid cultures of strain 4 were inoculated and grown in 40 ml rMB as described in section 3.1. When the OD_{600} value of cultures was at 0.6, infection was conducted with phage isolate 1/4 using a MOI value of 10. Phages were allowed to adsorb at room temperature for 5 min, after which cells were washed twice by centrifugation at 3220 g, 4°C for 10 min to remove any remaining extracellular phages. Subsequently, the resulting cell pellet was resuspended in original volume of rMB, and growth was regularly monitored using a spectrophotometer. Samples of 1 ml were collected from cultures at time points of 70, 100, 120, 150 and 180 min post infection (p.i.), and centrifuged at 10 000 *g*, 4 °C for 10 min to separate cells from supernatant. Aliquots of 100 µl were collected by centrifugation, and titration was performed as described in section 3.4, using dilutions of 10^{-3} – 10^{-8}.

3.8 Viral protein visualization

Control and infected cultures of strain 4 were grown as described in section 3.1. Host cells were infected with phage isolate 1/4 using a MOI value of 10.0. Samples were taken at the time points mentioned in section 2.1, and cells were harvested by centrifugation at 10 000 *g*, 4 °C for 5 min For gel electrophoresis, two different samples were prepared after centrifugation: one using the supernatant, the other using the pellet. Firstly, extracellular proteins were precipitated using trichloroacetic acid (TCA), which was conducted by collecting 1 ml of supernatant and adding TCA to a final concentration of 10% (v/v). After incubation on ice for 30 min, the samples were centrifuged at 13 000 *g*, 4 °C for 30 min, after which the TCA was removed. The remaining precipitated proteins were then dissolved in 50 µl DNA loading buffer. After collection of the supernatant for TCA precipitation, the remaining cell pellet was resuspended in 200 µl of 20 mM Tris-HCl (pH 7.2), to which sample buffer was added. The samples made from the pellet show the proteins present intracellularly, thus giving a comparison to the previously mentioned samples made using only the supernatant.

Tris-glycine-SDS-PAGE (10%) gels were utilized for separation and visualization of proteins. The aforementioned samples were then loaded in total volumes of 20 µl with 1x sample buffer into gels (Supplemental Recipe 3A). In addition, an unstained Page Ruler protein ladder (Thermo Scientific) was used as a marker for determination of protein size, and purified phage was used for easier recognition of phage proteins. Gel

electrophoresis was performed using a voltage of 120 V for 15 min initially, after which the voltage was lowered to 90 V for 45 min Gels were stained by Coomassie blue (Supplemental Recipe 3C), and imaged with BioRad ChemiDoc Imager.

3.9 Transmission EM

Sample preparation for transmission electron microscopy (TEM) was conducted by growing and infecting cultures as described in section 3.7. Samples of 3 ml were taken from infected and mock-infected cultures at time points of 0 , 15 , 30 , 60 , 120 , and 180 min p.i. After sampling, 25% glutaraldehyde (Sigma) was added so that the final concentration in sample was 2.5 % (v/v) in order to stabilize surface and intracellular structures. Samples were then incubated for 20 min at room temperature, and at +4 °C over night. The glutaraldehyde was washed away by centrifugation at 5000 *g* and 4 °C for 5 min and resuspending the remaining pellet to 0.5 ml of phosphate buffer. The cells were centrifuged one more time using the same settings, and the resulting pellet was stored in 0.5 ml of phosphate buffer on ice and taken for preparation of thin-layer cuts, conducted by The Electron Microscopy Unit of the Institute of Biotechnology, University of Helsinki. Imaging of the thin-layer cuts was done using a JEOL JEM-1400 microscope (Jeol Ltd., Japan), with a Gatan Orius SC 1000B CCD-camera (Gatan Inc., USA).

3.10 Total- and tRNA isolation

Total RNA was isolated from strain 4 cultures inoculated and grown in volumes of 100 ml as described in section 3.1. When the OD_{600} value reached 0.6, cultures were infected with phage isolate 1/4 and controls were mock-infected with rMB, as described in section 3.4. All cultures were grown at +15 °C with 200 rpm aeration. At each desired time point post-infection (p.i) (0, 15, 30, 60 and 120 min), a pair of infected and mock-infected culture bottles were taken, and cells were collected by centrifugation at 10 000 *g*, 4 °C for 5 min The resulting cell pellet was then resuspended in 10 ml of home-made Trizol (Supplemental Recipe 4A), after which the samples were incubated at room temperature for 20 min and frozen over night at -20 °C.

Cells resuspended in Trizol and stored at -20 °C were thawed on ice, and 100 µl of 1-bromo-3-chloropropane (BCP) was added per 1 ml of Trizol in sample. Acid-washed

glass beads were added in volumes of 2-3 ml to each, after which tubes were vortexed for 5 min and centrifuged at 10 000 *g* at room temperature for 15 min The resulting aqueous phase including RNA was collected, combined with 3 ml of Trizol and 600 µl of BCP, and treated as above with collection of the aqueous phase into fresh tubes. Acidic phenol (2x sample volume) and BCP (1/5 volume of phenol) were added to the samples, followed by strong vortexing for 5 min and centrifugation as above. The resulting RNA-containing aqueous phase was then collected into a separate tube. This step was repeated until the interphase was clear, and 2.5 sample volume of 99.6% ethanol was added for precipitation of RNA at -20 °C overnight. The concentration and quality of total RNA was determined using NanoDrop 2000 spectrophotometer (Thermo Scientific). Due to the ongoing pandemic, different batches of chemicals, such as phenol, had to be utilized during RNA isolation.

To isolate tRNA from total-RNA, Nucleobond AX-100 midi (Macherey-Nagel) columns were used. Recipes for used buffers included in Supplemental Recipe 4B. Total-RNA was resuspended in 10 ml of equilibration buffer (without Triton X-100), and columns were equilibrated with 10 ml of equilibration buffer including Triton X-100. The resuspended total-RNA was applied to the columns, followed by two washes using 12 ml of wash buffer. The wash buffer was tempered to 55 °C, which was maintained by applying the buffer to columns in volumes of 5 ml at a time. The first flowthrough from applying the total-RNA, along with the first two washes, were collected for analysis. Elutions of RNA bound to columns were conducted using 10 ml of elution buffers, first with buffer including 750 mM KCl, followed by buffer including 800 mM KCl, in order to ensure the collection of as much tRNA as possible. Each elution was collected into tubes containing 25 ml of 99.6% EtOH, and the tRNA was precipitated over night at -20 °C.

Following precipitation, the tRNA was pelleted by centrifugation at 10 000 *g*, 4 °C for 30 min. The resulting supernatant was removed and the pellet, including a large amount of salt, was washed with 80% EtOH. The tubes were centrifuged at 10 000 *g* and 4 °C for 5 min for subsequent washes. The resuling supernatant was discarded, and 80% EtOH was added in volumes of 25 ml for the first wash, and 10 ml for subsequent washes. Tubes were then placed in a rotator for 15 min at room temperature for proper resuspension of salt and tRNA, after which centrifugation was repeated. After all salt was removed the pellet was air-dried at room temperature for 10-30 min, until no moisture was visible, and

resuspended in 50 µl of sterile mQ-water. The concentration and quality of tRNA was measured using NanoDrop 2000 spectrophotometer (Thermo Scientific).

3.11 Quality of total-RNA and tRNA

Agarose gel electrophoresis was performed to confirm that the acquired total-RNA was intact and usable for tRNA isolation. A 1% agarose gel (w/v) in Tris-borate-EDTA (TBE) buffer was prepared, and samples with 500 ng of total-RNA were prepared with 1.5x denaturing loading dye (Supplemental Recipe 3C).

The quality of tRNA was confirmed using denaturing polyacrylamide-urea (PAA-U) gels (10%), into which 200 ng of tRNA was loaded from each sample collected during tRNA isolation descibed in section 3.10. Total volume of each sample was 20 µl after adding 2x RNA loading buffer (Supplemental Recipe 3B). A low range DNA marker (Thermo Fisher) was used for size reference. Gels were pre-run in 0.5x tris/Borate/EDTA (TBE) buffer for 20 min at 200 V, followed by loading of samples and running the gel electrophoresis for approximately 1.5 h at 200 V. Gels were stained using SYBR Gold Nucleic Acid Gel Stain (Thermo Fisher) and imaged with BioRad ChemiDoc Imager.

3.12 Sample preparation for mass spectrometry

Sample preparation was conducted firstly by digestion of tRNA into mononucleosides. Nuclease P1 (250 U/ml in 200 mM sodium acetate, pH 5.5; Sigma Aldrich) and Fast Alkaline Phosphatase (1 U/µl; Thermo Scientific) were diluted into sterile mQ for 10x dilutions. A master mix of enzymes was prepared, as described in Supplemental Recipe 4C. A minimum of 10 µg of tRNA was used for each sample, and the total volume in each reaction was adjusted to 19.8 µl with sterile mQ. Master mix was added to each sample in volumes of 10.2 µl, which were then incubated at 37 °C for 1.5 h. Following incubation, 15 µl of 0.5 M ammonium bicarbonate (NH_4HCO_3) was added and incubation was continued as above for 1 h. The reaction was then terminated by adding 5 µl of 5.0% trifluoroacetic acid (TFA) in mQ. The final volume was adjusted to 100 µl by addition of 0.1% TFA in H_2O, and 2 µl of $m^{1,3}\Psi$ (1,3-dimethylpseudouridine) nucleoside was added for internal spiking control.

Sample clean-up of cleaved nucleosides was performed using HyperSep Hypercarb SPE extraction tips (Thermo Scientific). Extraction tips were equilibrated by

applying 50 µl of 0.1% TFA in H_2O (mQ) into each tip and spinning at 875 *g* for 30 s. Equilibration was repeated five times. Afterwards, samples were applied to extraction tips in volumes of 50 µl at a time and spun as above. Subsequent washing was conducted five times using 50 µl of 0.1% TFA in H_2O and spun as above. Nucleosides were eluted with 50 µl of 0.1% TFA in 80% acetonitrile. The samples were centrifuged at 875 *g* for 1 min, after which a SpeedVac Concentrator (Savant) was utilized for sample drying at room temperature for 1.5 h – 2 h. Resulting nucleosides were resuspended in 40 µl of ammonium formate (NH_4HCO_2), pH 5.3, and the concentration was determined using a NanoDrop. Lastly, the final concentration was adjusted to 100 ng/µl with 5 mM ammonium formate.

3.13 Ultra-performance Liquid Chromatography Mass Spectrometry

Biological samples were analysed with Waters Aquity® UPLC system (Waters, Milford MA, USA) attached to Waters Synapt G2 HDMS mass spectrometer (Waters, Milford MA, USA) through an electrospray ionization (ESI) ion source. The rest of the UPLC-MS method was performed as described by Gregorová et al. (2020), using 50 ribonucleoside standards. Three independent replicates of the infected cultures were used for MS and subsequent data analysis.

3.14 Data analysis

MZmine2 software (version 2.40.1) (Pluskal et al., 2010) was utilized for generation of total ion (TIC) and extracted ion (XIC) chromatograms from .RAW format. A lookup list of ribonucleosides including data from Modomics regarding previously found $[M+H]^+$ and respective product ion masses was used for peak identification (Boccaletto et al., 2018). A database identification module included in MZmine2 was applied for peak identification, using the lookup list and information on retention time based on analysis of standards. The acquired peak intensities were normalized to non-natural nucleoside $m^{1,3}\Psi$ and averaged from three biological replicates.

3.15 Statistical analysis

Statistical analysis was performed using Microsoft Excel (Version 2106). To determine statistical significance of changes in modifications during the infection, a two-tailed, type 1 T-test was performed for each modification between infected samples and controls within the

same time point. Time points displaying p-values of ≤ 0.05 were considered statistically significant and observed further. Standard deviations from the average of three independent replicates are represented by error bars.

4 Results

4.1 Determining the amount of viable cells and infective phages

The number of viable cells was calculated using the formula in section 2.3. The acquired values for OD_{600} of 0.6 gave a resulting average of 3.07 x 10^8 cfu/ml (Table 1).

Transparent plaques were visible and counted after 2 nights after plating, based on which the titer of the produced phage agar-stock was calculated using the formula in section 2.4. The titer of the produced phage stock was calculated as 1.2 x 10^{11} pfu/ml.

Table 1: Calculated number of viable cells at different stages of growth

A_{600}	V.C. (cfu/ml)			Mean ± SD
0.5	3.45×10^8	2.88×10^8	2.01×10^8	$2.78 \times 10^8 \pm 0.752 \times 10^8$
0.55	3.16×10^8			
0.6	4.05×10^8	2.61×10^8	2.55×10^8	$3.07 \times 10^8 \pm 0.849 \times 10^8$
0.65	3.65×10^8			
0.7	3.32×10^8	3.59×10^8	3.23×10^8	$3.38 \times 10^8 \pm 0.187 \times 10^8$
0.75	4.00×10^8			

Values used to calculate average number of viable cells highlighted in a red box. Standard deviations calculated from the mean of three biological replicates.

4.2 Phage-host interaction and infection cycles

A range of MOI values was used to observe how the number of phages affects the infection cycle. Cell lysis occurs after 4-5 h at the lowest MOI values (Fig. 2A), while at values of 1.0 or higher it seems to occur between 2-3 h (Fig. 2B).

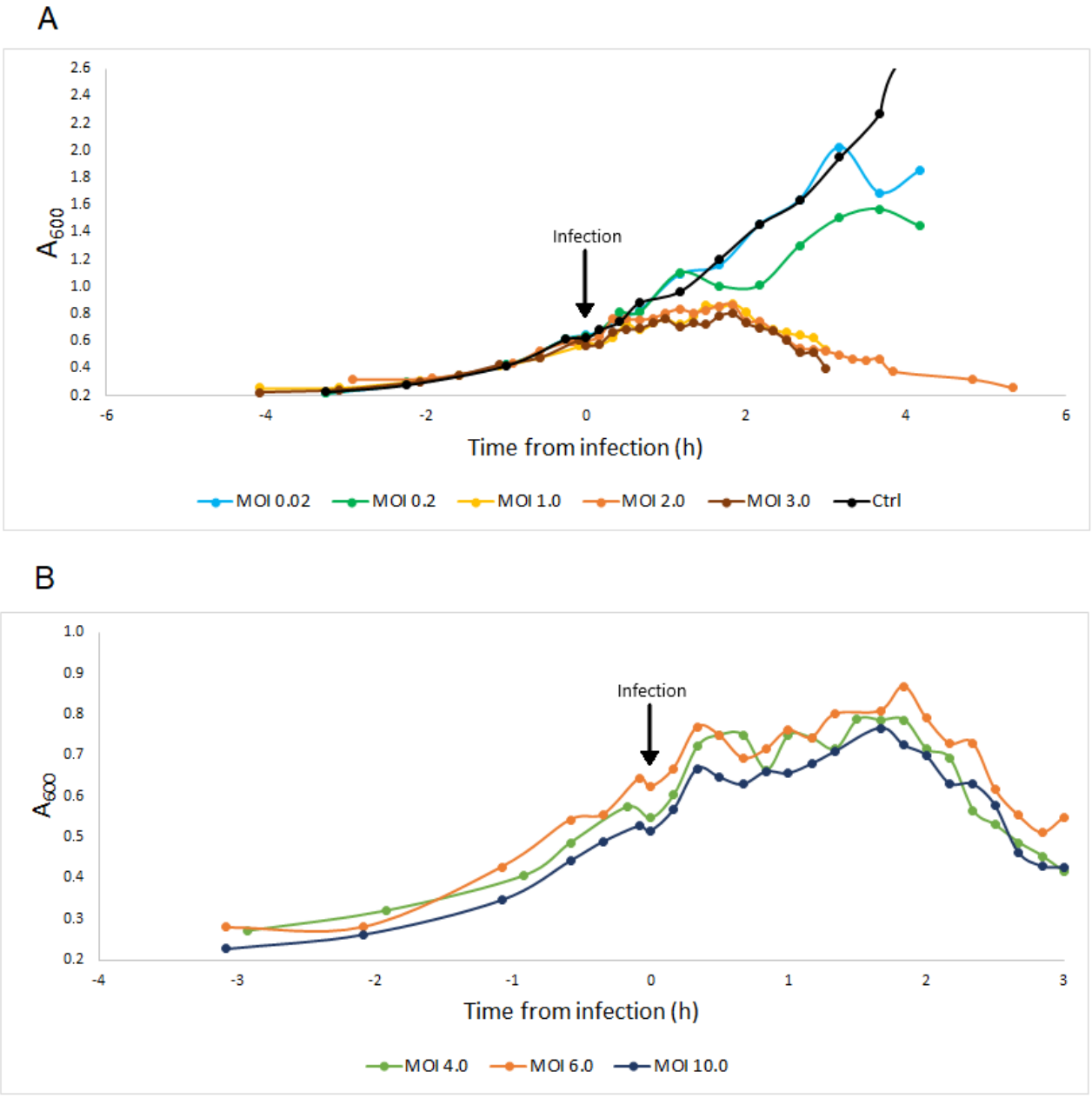

Figure 2: Growth curves for cultures infected with different amounts of phage. Curves of cultures infected with low MOI values in panel (A) and high MOI values in panel (B). Uninfected control included in panel (A) to illustrate strain 4 growth, applicable for comparison with all infected cultures. Point of infection marked with a black arrow. One of three replicates displayed for each MOI value, as time points differed between replicate measurements.

Respectively, the higher MOI values display growth similar to one another (Fig. 2). A reoccurring periodic incline and decline of host cell turbidity can be observed in every infected culture at every MOI value above 0.2, especially in cultures infected with a higher number of phages. This increase and decrease in turbidity follow a pattern of approximately 30 min long cycles, where the cell turbidity falls rapidly and recuperates shortly after. The final rapid

drop in cell turbidity occurs consistently between 2.5 and 3 h p.i. for cultures infected with MOI values above 0.2.

4.3 The amount of extracellular and intracellular phages

The amount of extracellular and intracellular phages throughout the infection cycle were investigated through plaque assay. The number of extracellular phages was initially high before removal of these by washing the cells (Fig. 3). The number of phages declined rapidly after washing and remained low until 2.5 h p.i. At this point, an increase in extracellular phages could be observed, which was followed by an even larger increase at 3 h p.i.

The number of intracellular phages underwent a steady increase during the infection (Fig. 3). At 2 h p.i., the number of intracellular phages was at its highest, after which the number dropped slightly when reaching the 3-hour time point.

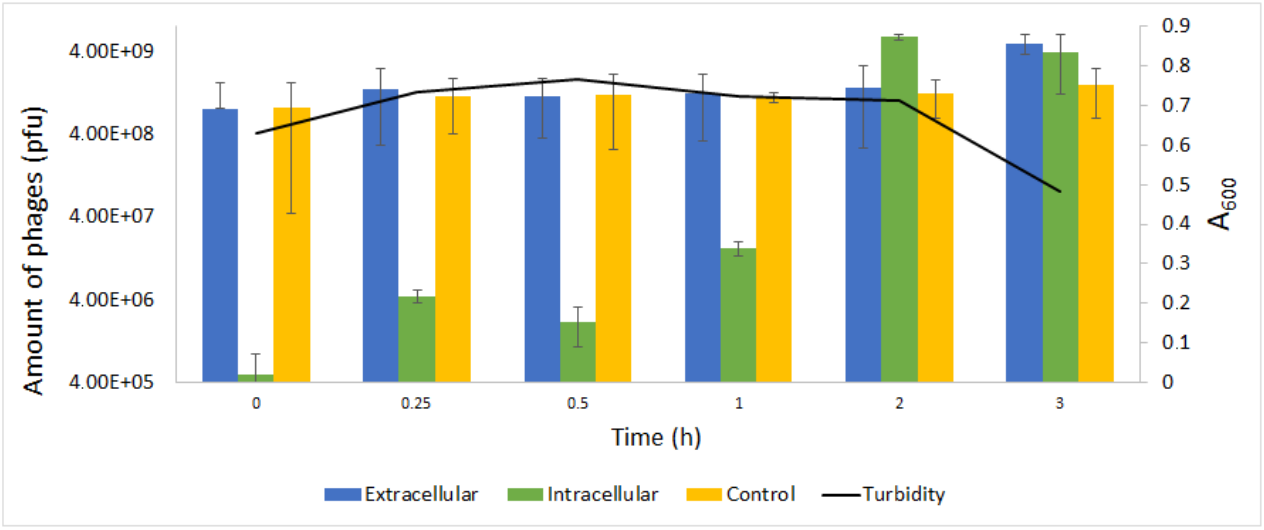

Figure 3: The amount of intracellular and extracellular phages over the course of infection. Black line represents cell turbidity. Left-side y-axis represents the amount of phages, visualized as coloured columns. Right-side y-axis represents absorbance at 600 nm wavelength, relevant for cell turbidity. X-axis represents the time p.i., with 0 being the moment of infection. Error bars represent standard deviation from the average of three biological replicates.

4.4 Showing viral protein production with gel electrophoresis

Protein components were investigated using gel electrophoresis using two differently made sets of samples for extracellular and intracellular proteins during the infection. Samples made using TCA precipitated proteins representing extracellularly present viral proteins showed a viral major capsid protein of size 37 kDa at time points 0 min, 150 min and 180 min, also seen in previous studies (Luhtanen et al., 2014; Senčilo et al., 2015) (Fig. 4A). Two other viral proteins were observable, with bands of sizes ~53 kDa and ~70 kDa, visible at the same time points, albeit vaguely at 0 min p.i., and not present in uninfected controls.

Samples made using cell pellet to represent intracellular proteins during the infection showed the same viral major capsid protein of size 37 kDa at time points 100 min, 150 min, and 180 min (Fig. 4B). The previously mentioned viral proteins of sizes ~53 kDa and ~70 kDa also had clear bands at the same time points.

4.5 Visualization of phage infection

Infected strain 4 cells were similar to uninfected controls at the point of infection (Fig. 5A). However, certain developments could be observed already at 15 min p.i., where denser material seen as a darker shade of grey could be seen occupying the space close to the membrane (Fig. 5B). Respectively, a lighter shade of grey, or even a white, was prevalent in the middle of the cell, which was not observed in uninfected controls. Similar changes were noticed in cells also at 30 min p.i. (Fig. 5C). At 60 min p.i., a small, denser coloring of dark grey was observed in some cells, especially by the cell membrane (Fig. 5D). In addition to denser grey, circular black spots were present in infected cells, which were not observed in uninfected cells. Similar observations were also made in infected cells at 120-minute time point, where the denser grey areas were numerous, consistent, and occurred more regularly than before (Fig. 5E). The number of these also increased between the 60-minute and 120-minute time points, in addition to a larger number of cells with circular black spots seen after 60 min p.i. Potential icosahedral heads of phages could also be seen inside cells at the 120-minute time point (Fig. 6).

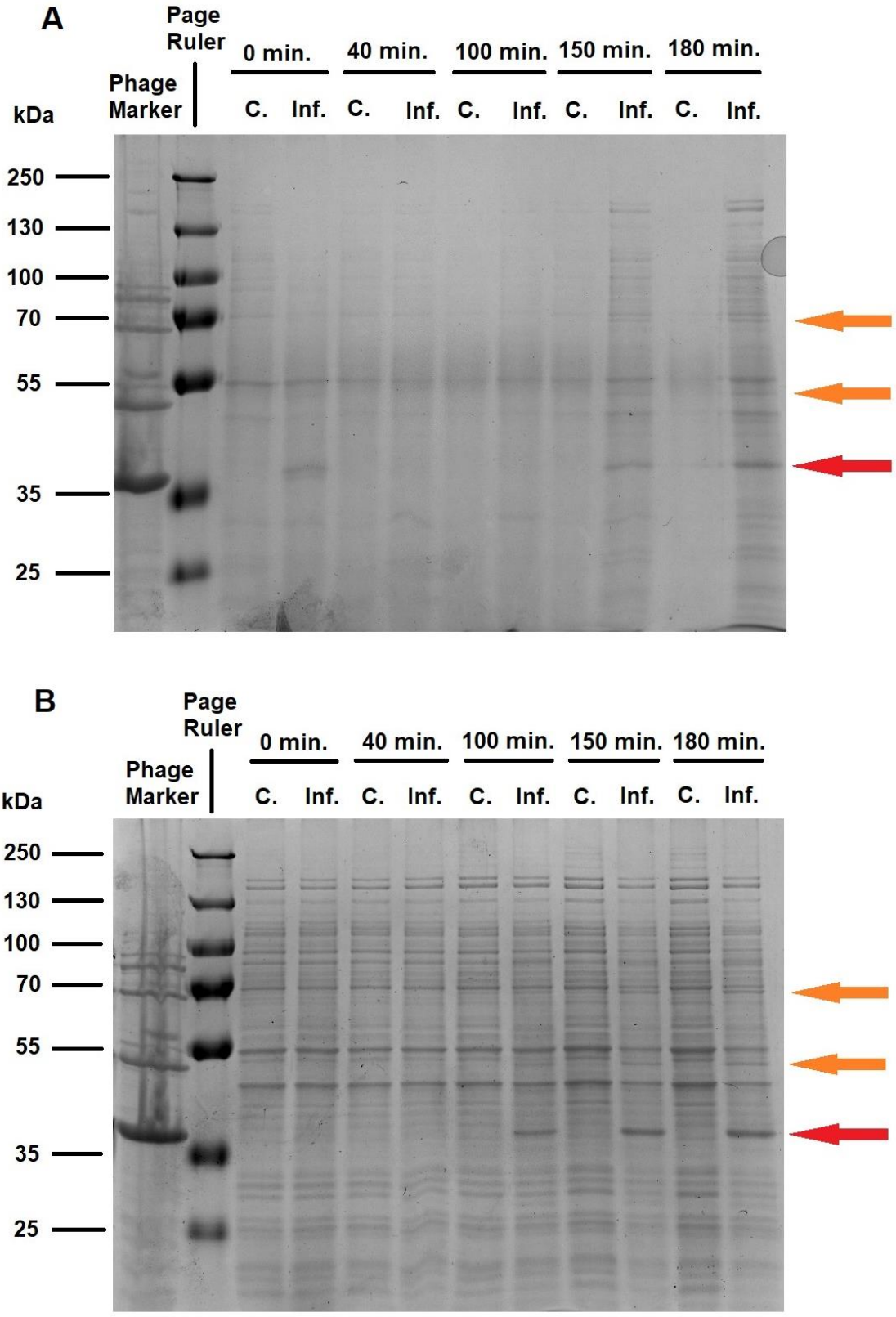

Figure 4: Protein patterns in SDS-PAGE. Samples made through (A) TCA precipitation and (B) from cell pellet show the viral major capsid protein at 37 kDa, highlighted with a red arrow. Wells with uninfected controls marked as “C” and wells with infected cultures marked as “Inf.”. Other viral proteins of sizes ~54 kDa and ~70 kDa indicated with orange arrows.

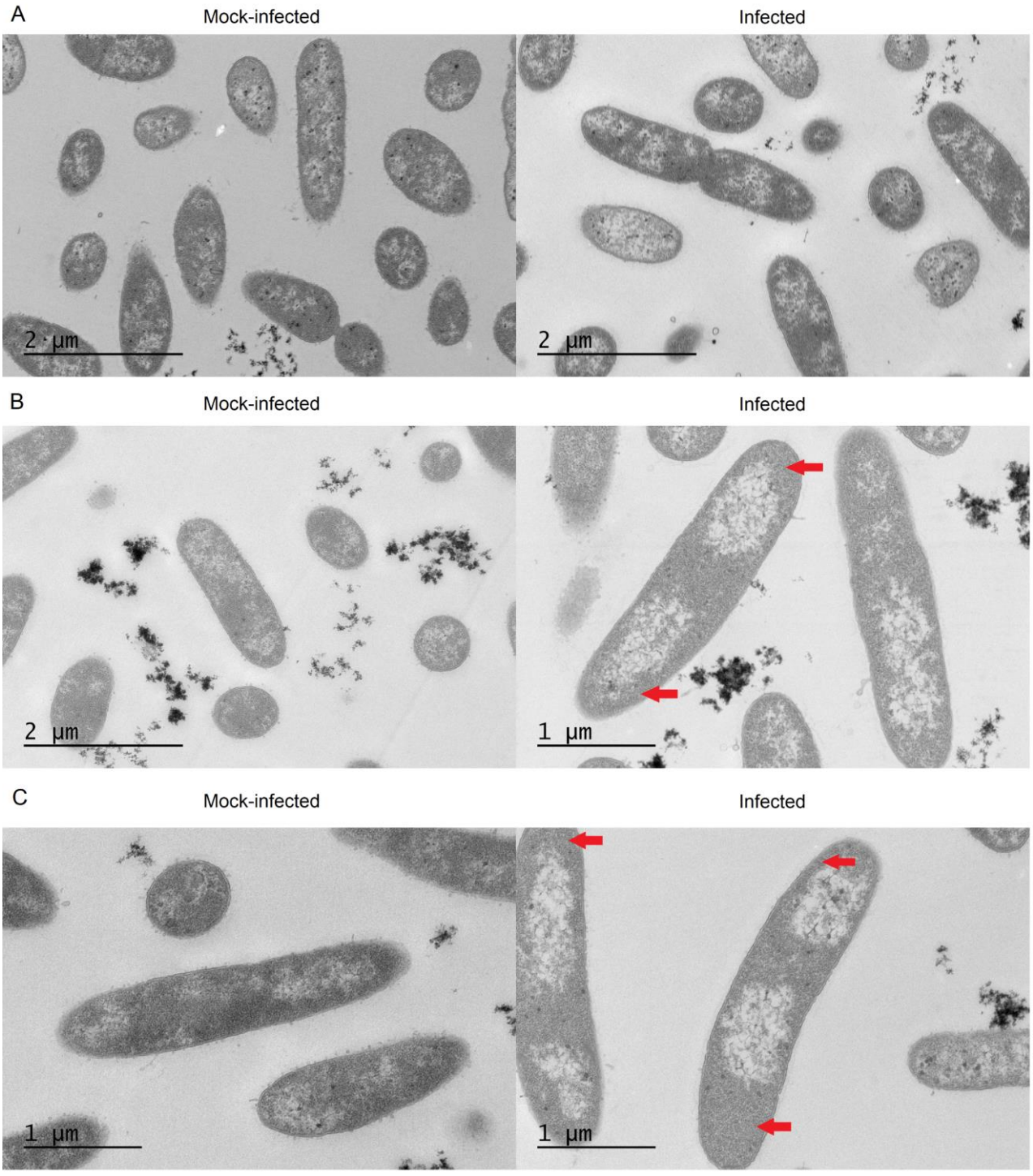
A
Mock-infected
Infected
2 µm
2 µm
B
Mock-infected
Infected
2 µm
1 µm
C
Mock-infected
Infected
1 µm
1 µm

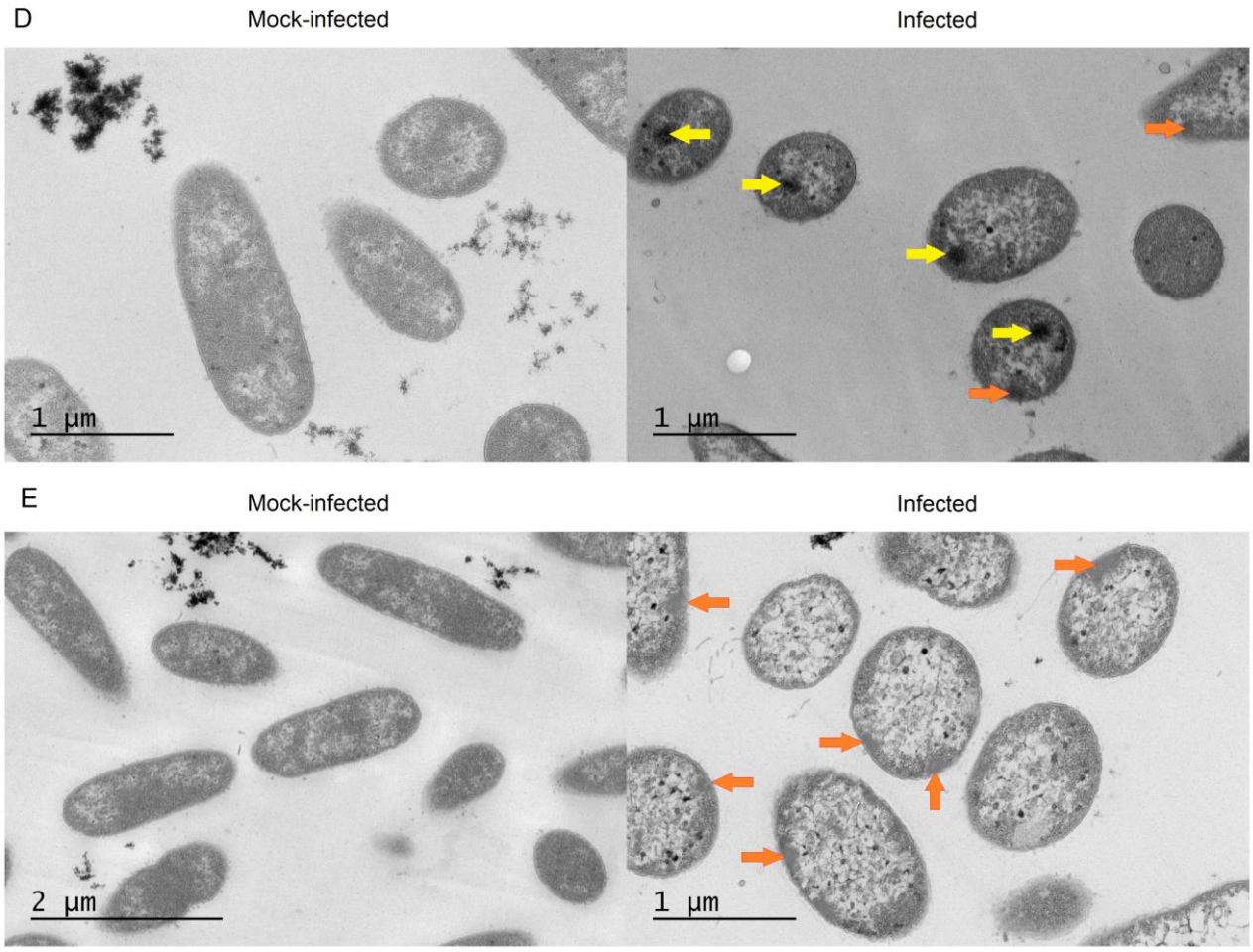

Figure 5: Transmission electron microscopy images of *Shewanella* sp. 4 cells and infected with phage isolate 1/4. Uninfected controls are on the left, infected cells on the right. Samples taken at different time points post-infection. (A) Moment of infection. (B) Cells at 15 min. post-infection. (C) Cells at 30 min. post-infection. (D) Cells at 60 min. post-infection. (E) Cells at 120 min. post-infection. Darker shades of grey around the cellular membrane marked with red arrows. Black spots marked with yellow arrows. Dense grey areas marked with orange arrows.

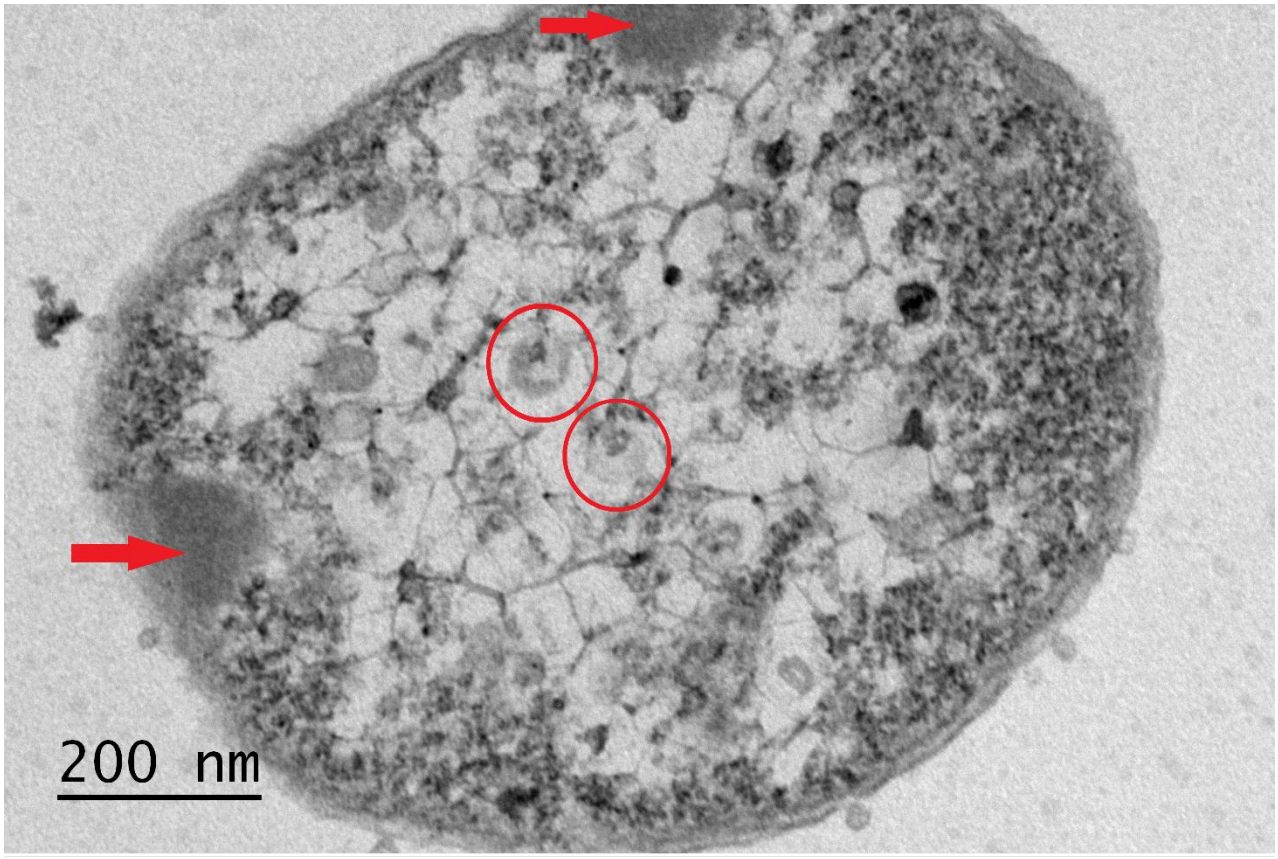

Figure 6: Transmission electron microscopy close-up image of an infected *Shewanella* sp. 4 cell 120 min. p.i. Possible icosahedral viral capsids highlighted in red circles. Denser grey areas highlighted with red arrows.

4.6 Quality of isolated RNA and tRNA

The quality of total- and tRNA was confirmed by agarose (1%) gel electrophoresis. The 23S, 16S, and 5S rRNAs (ribosomal RNA) were clearly observable reflecting the amount of RNA present (Fig. 7). Commonly, around 80% of bacterial, as well as mammalian, total-RNA consists of rRNA, which is why tRNA is not observable in agarose gels with total-RNA (Lodish et al., 2000; Scott et al., 2010).

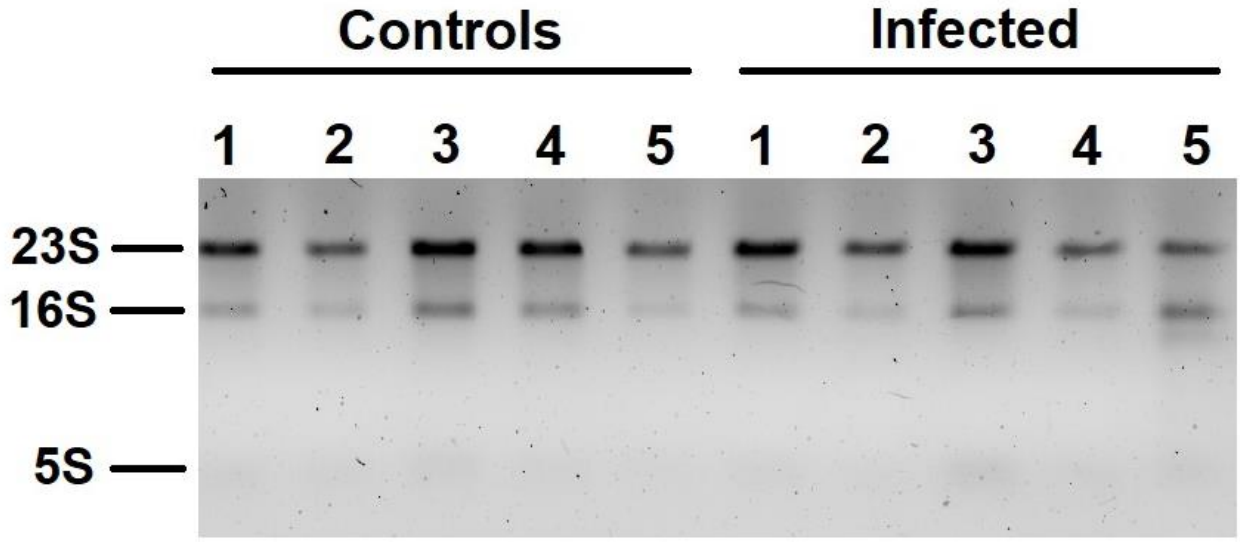

Figure 7: Representative gel of the quality of total-RNA analysed on agarose (1%) gel. Bacterial ribosomal RNAs marked on the left. Numbering on top represents time points of 0 min, 15 min, 30 min, 60 min, and 120 min p.i. Agarose gels made using replicate batches are shown in Supplemental Figure 1.

The quality of isolated tRNA was confirmed by PAA-U gel electrophoresis, where individual bands were clear and intact (Fig. 8). The tRNA present in the input consisting of previously extracted total-RNA shows the same tRNA bands as isolated tRNA samples, along with other RNAs accumulating at the top of the well due to size.

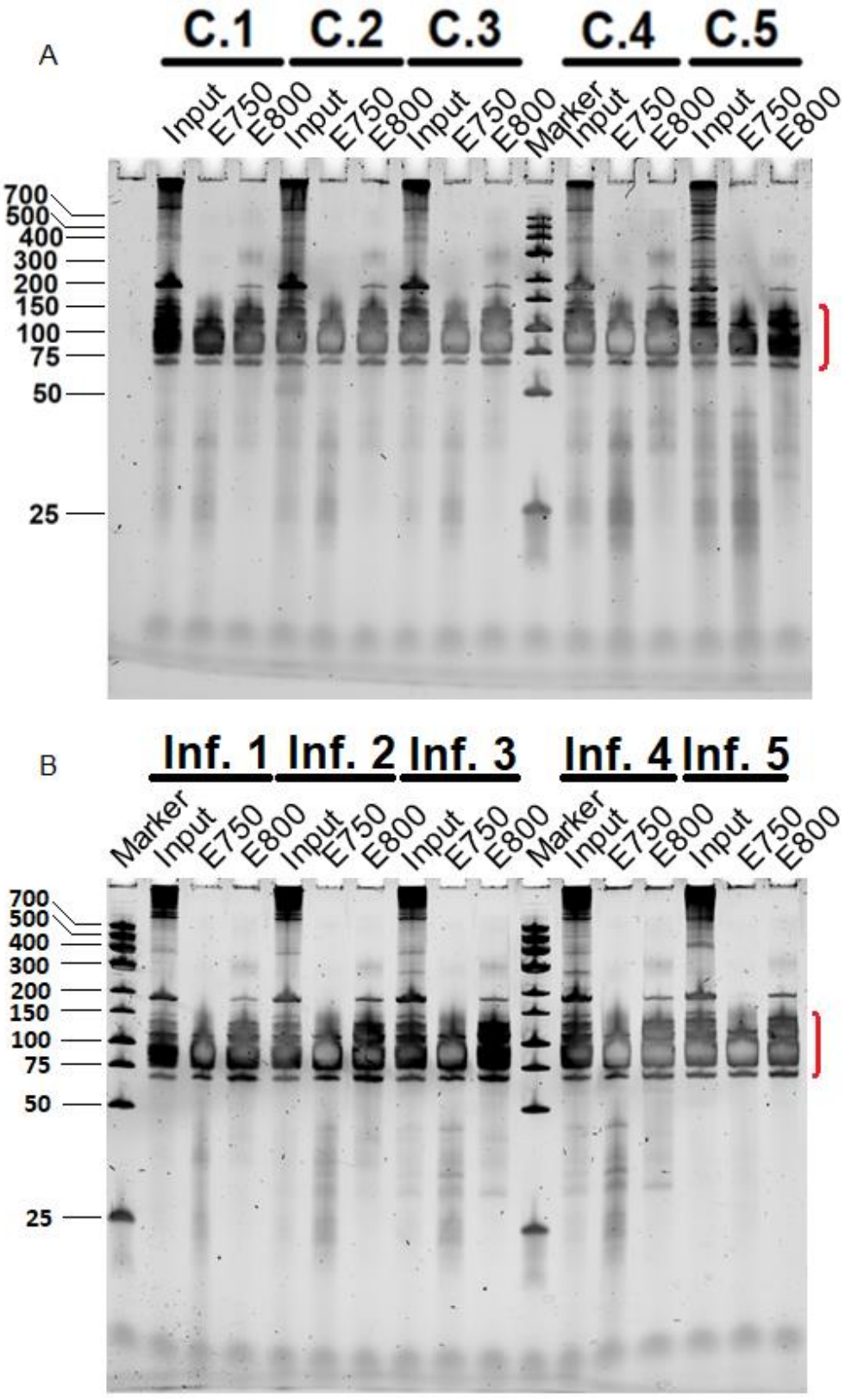

Figure 8: Quality of isolated tRNA in (A) uninfected and (B) infected samples, visualized on PAA-U gels. Inf. # represents samples taken from infected cultures and C. # from controls at time points of 0 min, 15 min, 30 min, 60 min, and 120 min p.i. Total-RNA used as input. Low range DNA marker used as ladder (Thermo Fisher). Concentrations of 750 mM and 800 mM KCl were used for eluting tRNA, marked as E750 and E800. tRNA cluster indicated with red brackets. PAA-u gels of replicate batches are shown in Supplemental Figure 2.

4.7 tRNA modifications

The identities of modified nucleosides found by UPLC-MS were determined by data analysis as described in section 3.14. Collectively, a total of 17 modifications were found in samples originating from both infected cultures and uninfected controls (Table 2).

Table 2: Identities of modified nucleosides

MODIFICATION	SYMBOL
2'-*O*-methylcytidine	Cm
5-carboxymethylaminomethyl-2-thiouridine	$cmnm^5s^2U$
dihydrouridine	D
N6-isopentenyladenosine	i^6A
1,3-dimethylpseudouridine	**$m^{1,3}\Psi$**
N1-methyladenosine	m^1A
N1-methylguanosine	m^1G
2-methyladenosine	m^2A
N5-methyluridine	m^5U
N6-methyladenosine	m^6A
N6-methyl-*N6*-threonylcarbamoyladenosine	m^6t^6A
N7-methylguanosine	m^7G
epoxyqueuosine	oQtRNA
queuosine	QtRNA
2-thiocytidine	s^2C
N6-threonylcarbamoyladenosine	t^6A
Pseudouridine	Ψ

Nucleoside identities, along with respective symbols, found collectively in all samples. Bolded non-natural nucleoside $m^{1,3}\Psi$ was used for normalization of intensities. Nomenclature and abbreviations according to the Modomics convention (Boccaletto et al., 2018).

The acquired data was first normalized and averaged between the three replicates. Statistical significance was seen at different time points for modifications m^1A, m^5U, and m^6t^6A, thus up- and downregulation of these nucleosides were analysed in more detail. Some changes in other modifications likely fall outside statistical significance due to peak intensity variance between samples. For nucleosides m^5U and m^1A, the t-test resulted in a value of <0.05 at only one time point each at 60 min and 120 min p.i. respectively. The fold change at these time points had a value of -1.238 for m^5U and -1.642 for m^1A. Meanwhile, nucleoside m^6t^6A had a p-value of <0.05 at time points 30 min and 60 min p.i., and a fold change of -1.202 and -1.584, respectively. Modification dynamics were investigated by calculating the fold change comparing infected and uninfected samples (Fig. 9). Modified nucleosides displaying statistical significance were all downregulated at the respective time points (Fig. 9A). Nucleoside Cm was also considered, despite its' change not displaying statistical significance, as a trend in changes of this modification was observable in all replicates. Moreover, Cm is also known to be altered during stress response. Here, Cm was upregulated at the second and third time points, leading to downregulation at the end of the infection cycle (Fig. 9B).

Changes in peak intensities of other nucleosides found in both infected and uninfected samples did not display statistical significance, remaining relatively stagnant throughout the experiment (Supplemental Figure 3).

A

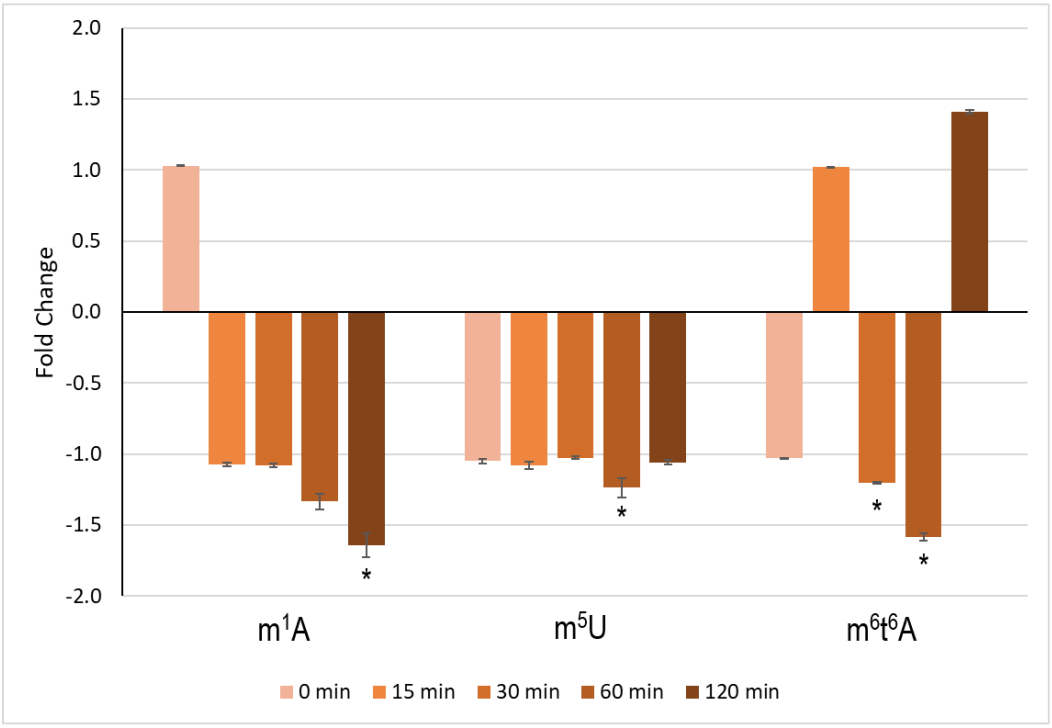

B

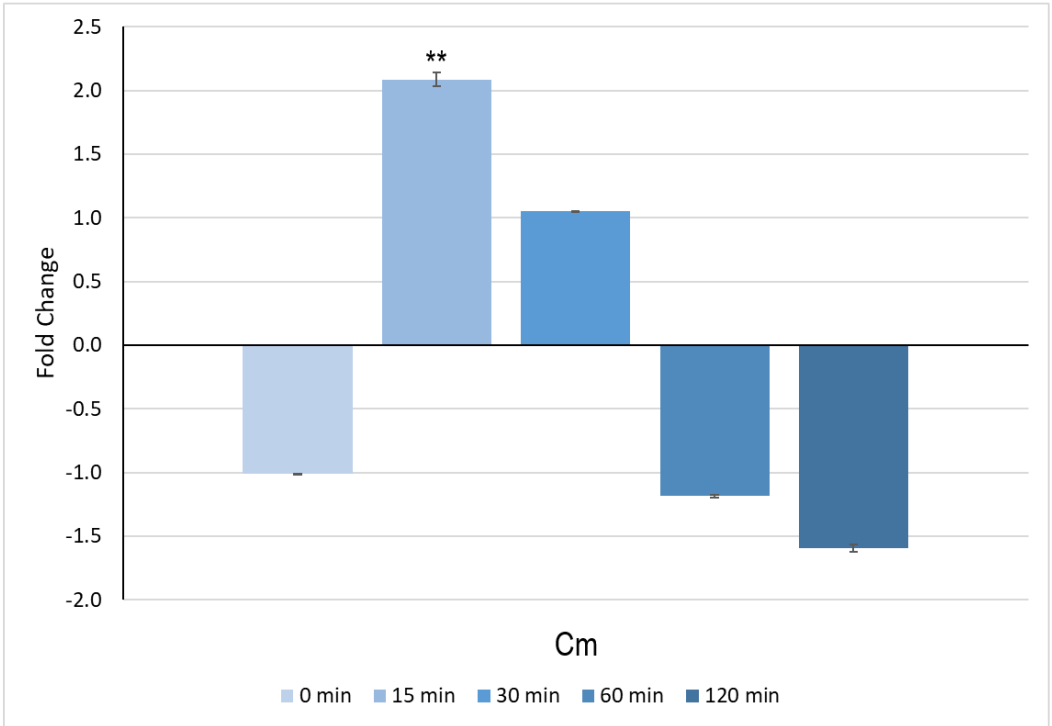

Figure 9: Fold change of (A) modified nucleosides displaying statistical significance, marked with a star (*=p<0.05) at the respective time point, and (B) nucleoside Cm, with the lowest p-value marked with two stars (**=p=0.286). Fold change describes the change in the m/z peak intensities of each nucleoside when comparing infected and uninfected samples. Fold change on the positive side and negative side of the x-axis signify an upregulation respective downregulation of the nucleoside modification.

5 Discussion

The Baltic Sea hosts a large variety of microorganisms, many of which have been previously characterized. However, algae and heterotrophic bacteria account for most of the currently characterized organisms (Kaartokallio, 2004; Kaartokallio et al., 2005; Mock & Thomas, 2005; Kaartokallio et al., 2008; Jørgensen et al., 2020). The unique brackish water of the Baltic Sea leads to the formation of equally unique ice composition, with variable thickness, extent, and distribution of nutrients (Granskog et al., 2006). Along with a unique and variable sea ice composition comes an equally fascinating combination of organisms dissimilar to the underlying sea water (Eronen-Rasimus et al., 2015). The isolation and cultivation of such organisms from sea ice, let alone their bacteriophages, had not been conducted and published until relatively recently (Luhtanen et al., 2014). Here, fundamental studies regarding the phage-host interactions between the psychrotrophic *Shewanella* sp. 4 and phage isolate 1/4 have been carried out to add to previously conducted research. Additionally, novel insights into the infection cycle and dynamics of tRNA nucleoside modifications during the infection are reported here.

Firstly, when growing strain 4 cultures, I wanted to investigate the similarity between rMB and previously published results acquired with ZoBell media (Luhtanen et al., 2014). Regardless of differences in media, strain 4 seemed to grow similarly on rMB as reported using ZoBell (Fig. 2) (Luhtanen et al., 2014; Senčilo et al., 2015). The cultures followed exponential growth characteristic for bacteria, when infection was not present, similar to results presented in previous research. As mentioned, only low MOI values were explored in previous studies, ranging from 0.2 to 5. I first investigated a similar range of MOI values to again confirm similarity between previously used media and the more defined one used in this project, which is rich in nutrients but otherwise resembles brackish water (Fig. 2). Furthermore, cells were infected using MOI values up to 10 to explore differences in cell growth depending on the number of phages used (Fig. 3). I found that the ensuing cell growth following infection is drastically different at the lowest MOI values of 0.02 and 0.2, where cell turbidity does not decline as rapidly as at higher values. Given the low number of phages infecting the cell culture, a comparatively low number of host cells were infected, leading to the uninfected host cells to continue normal growth. All MOI values above 0.2 displayed similar results, with rapid declination of cell turbidity starting at around 2 h p.i. A

MOI value of 10 has been commonly used for infection studies and was also chosen for this project for as simultaneous infection of host cells as possible.

As I wanted to see when new phages are produced, several experiments were conducted in conjunction. Firstly, a clear, steady increase in the number of intracellular phages after infection was illustrated by plaque assay, peaking at 2 h p.i. (Fig. 3). Initially, the number of phages is low as new infective virions have not been produced yet, meaning an equally low amount of viral proteins are present in host cells, and no protein bands are visible when conducting SDS-PAGE. Respectively, the number of extracellular phages did not increase or decrease during the infection cycle until the last time point (Fig. 3). A comparison between these results and the presence of viral proteins in and outside of host cells during different phases of infection shows how the production and accumulation of new phages occurs throughout the infection cycle (Fig. 4). Given the decrease in the number of intracellular phages and the optical density of the culture, and increase in extracellular ones, it is clear that a release of intracellular phages from host cells occurs at the last time point by lysis. When exploring viral protein release by SDS-PAGE, I can initially see some proteins present at the moment of infection as the cells have not been washed to remove any extracellular phages applied for the infection (Fig. 4A). However, no other viral protein bands are seen until the last two time points, indicating that viral proteins are indeed not released until the infection has progressed this far. Also, there are no visible viral protein bands at 100 min p.i. for extracellular proteins, but there is for intracellular ones, indicative of a high number of produced viral protein and presumably assembled phages just before lysis occurs. These results are also supported by changes in cell turbidity, as a declination is seen just as lysis occurs. To reiterate, all gathered evidence denotes the lytic pathway as the method of replication for phage 1/4. Thus, the lytic nature of phage 1/4 has been confirmed, with a period of approximately 3 h passing between the moment of infection and cell lysis.

Given the reproducibility and predictability of the infection cycle of phage 1/4, replication seems to be controlled and well-regulated. All infected cultures followed similar patterns when it came to cell turbidity, but a fascinating development arose when decreasing the amount of time between each measurement. Interestingly, a periodic incline and decline of cell turbidity was observed consistently for each infected culture, observable especially at higher MOI (Fig. 2). The amount of time between each fluctuation was also relatively consistent, with a duration of approximately 30 min. This behavior started at infection and could

be observed until cell lysis. However, during lysis it is difficult to distinguish between variance in the measurements, and the previously seen fluctuations. A similar phenomenon was seen previously while infecting *Shewanella* sp. 49 by phage 3/49, where a partial drop followed by an increase in cell turbidity was seen at high MOI values (Senčilo et al., 2015). This result was attributed to premature lysis and subsequent infection of uninfected cells based on the low number of extracellular phages present until lysis. However, in my experiments, given the increasing number of phages as shown by plaque assay and SDS-PAGE, infective virions do not appear to be released during mid-stages of the infection (Fig. 3, Fig. 4). These results indicate that no premature lysis occurs during the infection (Fig. 3). Instead, the increasing number of intracellular phages during the infection indicates a steady buildup of phage particles and assembly of new phages within the host cell, leading to release at around 3 h p.i. (Fig. 3). Thus, it is evident that the reoccurring fluctuations in cell turbidity during the early-to-mid stages of infection are not caused by cellular lysis, but by some other factor. Furthermore, considering each infected strain 4 culture displayed similar behavior in terms of cell turbidity, while uninfected controls did not, it seems unlikely that the fluctuations are the result of an error, human or technical. Generally, these results indicate that the infection does indeed follow a common lytic pathway with specific steps: initial infection, viral genome translation, intracellular viral component production, and release of new phages by cell lysis (Clokie et al., 2011). Regardless, the observed periodic incline and decline of cell turbidity is a phenomenon worth future investigation as the cause remains a speculation.

In spite of the infection cycle of phage 1/4 having been studied before, intracellular changes and rearrangements occurring in host cells as a result of the infection have remained to be properly investigated. TEM showed that a density disparity in the intracellular structures becomes evident between the infected cells and controls already at 15 min p.i. (Fig. 5B). This development became more consistent over time, resulting in the disparity becoming the norm rather than an exception (Fig. 5C). Similar occurrence has been previously documented in *Bacillus subtilis*, where virus protein production becomes compartmentalized during the infection (Labarde et al., 2021). The roundish black spots observed at 60 min p.i. were an interesting phenomenon, as these were absent at earlier time points (Fig. 5D). Additionally, the regularity of these also increased at the last time point, where the occurrence of denser grey areas at the cell membrane became a common feature (Fig. 5E).

Indeed, it seems that a certain compartmentalization takes place during the infection, leading to visible alterations in structure. Previously, the compartmentalization of viral proteins within host cells has been observed to enclose essential enzymatic reactions, as well as storage of viral particles (Labarde et al., 2021). Currently, however, the specific mechanism in the strain 4-phage 1/4 pair remains a speculation, as such compartmentalization has not yet been confirmed. Potential icosahedral viral capsids could also be observed in close-up images of infected cells at 120 min p.i. (Fig. 6). As viral proteins have already been accumulated at this time point, along with the lysis occurring soon after, it is likely the observed structures are indeed viral capsids. Additionally, similar structures were not seen at any of the previous time points, further adding to the likelihood of these being phage capsids. Also, when comparing the controls at different time points it is apparent that no changes appear as a result of normal cell growth. However, some of the infected cells displayed behavior similar to uninfected ones. The inconsistencies, such as the lack of a regular distribution of different densities of grey, could be explained with cell orientation in the sample. As thin-layer samples were utilized, the imaging essentially captured only a two-dimensional cut of the culture. An additional possibility is the absence of infection in all host cells, which may occur regardless of the MOI value used. Not all cells will be infected immediately at the time of infection, as phages rely on Brownian motion for motility, and may adsorb to the same host cells (Gustafsson et al., 2018).

It has been previously reported that regulating translation through post-transcriptional tRNA modifications is an essential part of the cellular stress response in a variety of organisms (Koh & Sarin, 2018). Optimal translation of key stress response transcripts is a necessity to ensure cell viability, or at the very least survival, in unfavorable conditions (Gu et al., 2014). Thus, the dynamic nature of more than 150 tRNA modifications constitutes a versatile defense system in bacteria to combat stress factors such as rapid environmental changes, or pathogenic infection (Boccaletto et al., 2018). Environmental stressors affect the tRNA epitranscriptome by either altering modifications in mature tRNA, or by upregulation and/or inactivation of tRNA-modifying enzymes (Edwards et al., 2020). Viral infections themselves cause significant stress in the infected host cell, although potential links to utilization of tRNA modifications for infection efficiency have also been speculated to be a result of a long-lasting, continuous arms race and coevolution. Here I found 16 modified nucleosides in *Shewanella* sp. 4 infected by phage 1/4 (Table 2). The relative amounts of three

modifications were found to be significantly altered during the infection, requiring more intricate analysis. The m^1A modification displayed intriguing behavior by firstly being upregulated at the moment of infection but experiencing increasing downregulation over the course of the infection (Fig. 9). Previously it has been shown that m^1A modification has different effects depending on the position on the tRNA molecule (Oerum et al., 2017). Modifications m^1A_9 and m^1A_{58} have been extensively studied, and found to contribute to structural stability, thermostability, and/or correct folding of the tRNA molecule (Horie et al., 1985; Helm et al., 1998). Interestingly, the modification m^1A_{58} in human $tRNA^{Lys}_3$ has also been linked to the efficiency of retroviruses by contributing to reverse transcription fidelity (Auxilien et al., 1999). As the modification is heavily downregulated at the last time point during infection of strain 4, one could speculate that destabilization of tRNA occurs as a result of the infection. Perhaps a less stable tRNA structure is in this case favorable for viral particle production, and thus gives an advantage to the bacteriophage.

Similar to the modification m^1A, m^5U is also downregulated during the entire infection cycle (Fig. 9). However, in contrast to m^1A, the m^5U modification has been found in abundance in psychrophiles (Dalluge et al., 1997). Previous studies have shown that m^5U_{54} hypomodification induces the formation and accumulation of tRNA-derived small RNAs (tsRNAs) by cleavage of tRNA near the anticodon (Pereira et al., 2021). Additionally, subjection to conditions inducing oxidative stress leads to m^5U hypomodification, and thus also accumulation of tsRNAs. A correlation between m^5U hypomodification and cellular stress response may present a possible reason to the downregulation of said modification during the infection of strain 4 by phage 1/4.

Akin to the previously discussed modifications, m^6t^6A shows significant downregulation at 30 min and 60 min p.i. (Fig. 9). Oddly, the upregulation of said nucleoside, especially at the last time point, does not seem feasible and may be the result of a replicate displaying an abnormally large variance. However, downregulation of m^6t^6A seems to correlate with previously conducted research, as the modification has an important role in translational accuracy and codon recognition (Helm & Alfonzo, 2014; Zheng et al., 2017). Utilization by phage 1/4 during the infection of *Shewanella* sp. 4 for decreased translational accuracy and recognition of viral codons seems to be a reasonable possibility, given the location of said modification at the anticodon loop of tRNA and its' role in translation. In addition, m^6t^6A modification is evolutionarily conserved throughout all organisms, having a role in start

codon recognition for ANN codons, which could indicate utilization by different types of viruses as well (Lin et al., 2018).

Unlike the selected interesting tRNA modifications presented above, the modification Cm did not display statistical significance at any time point. However, as said modification has been previously linked to oxidative stress, and goes through fascinating up- and downregulation, analysis of acquired results was deemed beneficial (Fig. 9B). An increase of several modifications, including Cm_{32}, has been found to occur when *Saccharomyces cerevisiae* cells are exposed to hydrogen peroxide, leading to oxidative stress response (Chan et al., 2010). Similar stress response may be a possibility in the infection of strain 4, as we see the modification upregulated at the second time point (Fig. 9B). However, statistical significance could not be shown due to variance in peak intensities between the replicates, despite an observable trend. Additionally, if such a stress response is indeed induced, the modification is downregulated at later stages of the infection, indicating dynamic nature of infection-induced responses.

Certain conclusions, albeit requiring further proof and replication, can be drawn from the discovered alterations to highlighted tRNA modifications to the interaction between strain 4 and phage 1/4. Structural stability, translational accuracy, and codon usage seem to be some of the probable candidates for effects taken advantage of by phage 1/4. However, speculation is relatively limited as most tRNA modifications discovered in infected cultures and uninfected controls remained stable throughout the infection (Supplemental Figure 3). Also, different modified nucleosides ionize with different efficiency, meaning some will display with higher prevalence. Electrospray ionization limits the quantification to a relative comparison, while a more detailed investigation regarding the molar amount of each nucleoside would require absolute quantification. However, a need for this rarely arises, as most experiments give comparable results, for example between uninfected and infected cultures. In this case, knowing the absolute amounts is less relevant than the changes occurring between the observed results. Additionally, absolute quantification would be possible only through calibration of equipment using nucleoside standards, which is not feasible in this case as not all of said standards are available. As certain psychrophiles have been shown to contain higher amounts of specific nucleosides, it may be beneficial to consider such an experiment in future studies (Dalluge et al., 1997). However, due to the ongoing pandemic the issues with chemical supplies led to a situation where different batches had to be utilized

for the purpose of the results presented in this project. It is likely that reproduction of protocols using only one batch of each chemical would yield less variance in results, and statistical significance could be discovered in modifications not considered here. Additionally, the odd variance in up- and downregulation of modifications could possibly be avoided by accurate replication, making the results acquired by UPLC-MS more reliable.

6 Conclusion

In summary, the fundamental understanding of the infection cycle of phage 1/4 when infecting *Shewanella* sp. 4 was reached as intended, including investigating the production and release of new phages and cellular growth, both uninfected and infected.

Results regarding the dynamic phage-host interactions, along with tRNA-modificational changes, have provided insight and expanded our understanding of this phage-host pair. If such a novel bacteria and bacteriophage was to be utilized in further research, a foundational understanding of their respective interactions and characteristics is essential. Moreover, if *Shewanella* sp. 4 is confirmed to contribute to the spoilage of fishery products and bioremediation as believed, these results will be a valuable asset for related industry and continued research. Until then, however, the details of the infection cycle, including the inclining and declining cell turbidity, should be investigated further. Additionally, the specific intracellular components seen in TEM may be worth additional studies, as these seem to be directly caused by the infection. Lastly, discovering significance in other modified nucleosides may affirm the functions of the ones highlighted in this project, and how the bacteriophage may utilize them during the infection. Future research could include investigating vtRNA expression and modifications, along with studying translation more intricately, with focus on observing whether the translated proteins are of the type that would benefit from a changed codon usage due to modifications. The utilization of these tRNA modifications could thus be connected to the virus and its' infection of the host. To conclude, understanding the effects of post-transcriptional tRNA modifications on stress response and metabolic regulation, and their role in cell survival, provides a foundation for future research, not only for basic science, but also for industry, and potential clinical applications.

7 Acknowledgements

Dr Mirka Lampi and Dr Peter Sarin are thanked for providing extensive supervision and assistance throughout the project. The author also thanks Pavlína Gregorová for help with RNA isolation, and the entire RNAcious laboratory team for their input, aid, and comments. The Electron Microscopy Unit of the Institute of Biotechnology, University of Helsinki, is thanked for providing laboratory facilities.

8 References

Agris, P.F., Vendeix, F.A.P., and Graham, W.D. (2007). tRNA's Wobble Decoding of the Genome: 40 Years of Modification. J Mol Biol 366, 1-13.

Auxilien, S., Keith, G., Le Grice, S.F., and Darlix, J.L. (1999). Role of post-transcriptional modifications of primer tRNALys,3 in the fidelity and efficacy of plus strand DNA transfer during HIV-1 reverse transcription. J Biol Chem 274, 4412-4420.

Boccaletto, P., Machnicka, M.A., Purta, E., Piatkowski, P., Baginski, B., Wirecki, T.K., de Crécy-Lagard, V., Ross, R., Limbach, P.A., Kotter, A., Helm, M., and Bujnicki, J.M. (2018). MODOMICS: a database of RNA modification pathways. 2017 update. Nucleic Acids Res 46, D303-D307.

Boo, S.H., Kim, Y.K. (2020). The emerging role of RNA modifications in the regulation of mRNA stability. Exp Mol Med 52, 400–408.

Breitbart, M. (2012). Marine viruses: truth or dare. Ann Rev Mar Sci 4, 425-448.

Bushell, M., and Sarnow, P. (2002). Hijacking the translation apparatus by RNA viruses. J Cell Biol 158, 395-399.

Campoy, S., Hervàs, A., Busquets, N., Erill, I., Teixidó, L., and Barbé, J. (2006). Induction of the SOS response by bacteriophage lytic development in Salmonella enterica. Virology 351, 360-367.

Chan, C.T.Y., Dyavaiah, M., DeMott, M.S., Taghizadeh, K., Dedon, P.C., and Begley, T.J. (2010). A Quantitative Systems Approach Reveals Dynamic Control of tRNA Modifications during Cellular Stress. PLoS Genet 6, e1001247.

Clokie, M.R., Millard, A.D., Letarov, A.V., and Heaphy, S. (2011). Phages in nature. Bacteriophage 1, 31-45.

Crick, F.H. (1966). Codon—anticodon pairing: the wobble hypothesis. J Mol Biol 19(2), 548-555.

Dalluge, J.J., Hamamoto, T., Horikoshi, K., Morita, R.Y., Stetter, K.O., and McCloskey, J.A. (1997). Posttranscriptional modification of tRNA in psychrophilic bacteria. J Bacteriol 179, 1918-1923.

Dedon, P.C., and Begley, T.J. (2014). A system of RNA modifications and biased codon use controls cellular stress response at the level of translation. Chem Res Toxicol 27, 330-337.

Dendooven, T., Van den Bossche, A., Hendrix, H., Ceyssens, P., Voet, M., Bandyra, K.J., De Maeyer, M., Aertsen, A., Noben, J., Hardwick, S.W., Luisi, B.F., and Lavigne, R. (2017). Viral interference of the bacterial RNA metabolism machinery. RNA Biol 14, 6-10.

Dreher, T.W. (2009). Role of tRNA-like structures in controlling plant virus replication. Virus Res 139, 217-229.

Dreher, T.W. (2010). Viral tRNAs and tRNA-like structures. Wiley Interdiscip Rev RNA 1(3), 402-414.

Dy, R.L., Richter, C., Salmond, G.P.C., and Fineran, P.C. (2014). Remarkable Mechanisms in Microbes to Resist Phage Infections. Annu Rev Virol 1, 307-331.

Edwards, A.M., Addo, M.A., and Dos Santos, P.C. (2020). Extracurricular Functions of tRNA Modifications in Microorganisms. Genes (Basel) 11, 907.

Endres, L., Dedon, P.C., and Begley, T.J. (2015). Codon-biased translation can be regulated by wobble-base tRNA modification systems during cellular stress responses. RNA Biol 12, 603-614.

Eronen-Rasimus, E., Lyra, C., Rintala, J., Jürgens, K., Ikonen, V., and Kaartokallio, H. (2015). Ice formation and growth shape bacterial community structure in Baltic Sea drift ice. FEMS Microbiol Ecol 91, 1-13.

Granskog, M., Kaartokallio, H., Kuosa, H., Thomas, D.N., and Vainio, J. (2006). Sea ice in the Baltic Sea – A review. Estuar Coast Shelf Sci 70, 145-160.

Gregorova, P., Sipari, N.H., and Sarin, L.P. (2020). Broad-range RNA modification analysis of complex biological samples using rapid C18-UPLC-MS. RNA Biol 1-8.

Gu, C., Begley, T.J., and Dedon, P.C. (2014). tRNA modifications regulate translation during cellular stress. FEBS Lett 588, 4287-4296.

Gustafsson, O., Gustafsson, S., Manukyan, L., & Mihranyan, A. (2018). Significance of Brownian Motion for Nanoparticle and Virus Capture in Nanocellulose-Based Filter Paper. Membranes 8(4), 90.

Hampton, H.G., Watson, B.N.J., and Fineran, P.C. (2020). The arms race between bacteria and their phage foes. Nature 577, 327-336.

Hanlon, G.W., Denyer, S.P., Olliff, C.J., and Ibrahim, L.J. (2001). Reduction in exopolysaccharide viscosity as an aid to bacteriophage penetration through Pseudomonas aeruginosa biofilms. Appl Environ Microbiol 67, 2746-2753.

Helm, M., Brulé, H., Degoul, F., Cepanec, C., Leroux, J.P., Giegé, R., and Florentz, C. (1998). The presence of modified nucleotides is required for cloverleaf folding of a human mitochondrial tRNA. Nucleic Acids Res 26, 1636-1643.

Helm, M., and Alfonzo, J.D. (2014). Post-transcriptional RNA modifications: Playing metabolic games in a cell's chemical legoland. Chem Biol 21, 174-185.

Holmfeldt, K., Titelman, J., and Riemann, L. (2010). Virus production and lysate recycling in different subbasins of the northern Baltic Sea. Microb Ecol 60, 572-580.

Horie, N., Hara-Yokoyama, M., Yokoyama, S., Watanabe, K., Kuchino, Y., Nishimura, S., and Miyazawa, T. (1985). Two tRNAIle1 species from an extreme thermophile, Thermus thermophilus HB8: effect of 2-thiolation of ribothymidine on the thermostability of tRNA. Biochemistry 24, 5711-5715.

Horvath, P., and Barrangou, R. (2010). CRISPR/Cas, the immune system of bacteria and archaea. Science 327, 167-170.

Jin, M., He, T., and Zhang, X. (2019). Marine Microbe Stress Responses to Bacteriophage Infection. Virus Infection and Tumorigenesis: Hints from Marine Hosts' Stress Responses (Zhang, X. Ed.). Singapore. Springer. pp 141-174.

Jørgensen, B.R., and Huss, H.H. (1989). Growth and activity of Shewanella putrefaciens isolated from spoiling fish. Int J Food Microbiol 9, 51-62.

Jørgensen, B.B., Andrén, T., and Marshall, I.P.G. (2020). Sub-seafloor biogeochemical processes and microbial life in the Baltic Sea. Environ Microbiol 22, 1688-1706.

Kaartokallio, H. (2004). Food web components, and physical and chemical properties of Baltic Sea ice. Mar Ecol Prog Ser 273, 49-63.

Kaartokallio, H., Laamanen, M., and Sivonen, K. (2005). Responses of Baltic Sea Ice and Open-Water Natural Bacterial Communities to Salinity Change. Appl Environ Microbiol 71, 4364-4371.

Kaartokallio, H., Tuomainen, J., Kuosa, H., Kuparinen, J., Martikainen, P.J., and Servomaa, K. (2008). Succession of sea-ice bacterial communities in the Baltic Sea fast ice. Polar Biol 31, 783-793.

Kasman, L.M., and Porter, L.D. (2020). Bacteriophages. StatPearls. Treasure Island. StatPearls Publishing.

Koh, C., & Sarin, L.P. (2018). Transfer RNA modification and infection – Implications for pathogenicity and host responses. Biochim Biophys Acta Gene Regul Mech 1861(4), 419-432.

Labarde, A., Jakutyte, L., Billaudeau, C., Fauler, B., López-Sanz, M., Ponien, P., Jacquet, E., Mielke, T., Ayora, S., Carballido-López, R., and Tavares, P. (2021). Temporal compartmentalization of viral infection in bacterial cells. Proc Natl Acad Sci USA 118, e2018297118.

Labrie, S.J., Samson, J.E., and Moineau, S. (2010). Bacteriophage resistance mechanisms. Nat Rev Microbiol 8, 317-327.

Li, S. (2019). Regulation of Ribosomal Proteins on Viral Infection. Cells, 8(5), 508.

Lin, H., Miyauchi, K., Harada, T., Okita, R., Takeshita, E., Komaki, H., Fujioka, K., Yagasaki, H., Goto, Y., Yanaka, K., et al. (2018). CO2-sensitive tRNA modification associated with human mitochondrial disease. Nat Commun 9, 1875.

Liu, B., Wu, S., Song, Q., Zhang, X., and Xie, L. (2006). Two novel bacteriophages of thermophilic bacteria isolated from deep-sea hydrothermal fields. Curr Microbiol 53, 163-166.

Lodish, H., Berk, A., Zipursky, S.L., et al. (2000). Molecular Cell Biology. 4th edition. New York. W. H. Freeman. Section 11.6.

Luhtanen, A., Eronen-Rasimus, E., Kaartokallio, H., Rintala, J., Autio, R., and Roine, E. (2014). Isolation and characterization of phage-host systems from the Baltic Sea ice. Extremophiles 18, 121-130.

Luhtanen, A., Eronen-Rasimus, E., Oksanen, H.M., Tison, J., Delille, B., Dieckmann, G.S., Rintala, J., and Bamford, D.H. (2018). The first known virus isolates from Antarctic sea ice have complex infection patterns. FEMS Microbiol Ecol 94.

Lyons, S.M., Fay, M.M., and Ivanov, P. (2018). The role of RNA modifications in the regulation of tRNA cleavage. FEBS Lett 592, 2828-2844.

Marchand, I., Nicholson, A.W., and Dreyfus, M. (2001). Bacteriophage T7 protein kinase phosphorylates RNase E and stabilizes mRNAs synthesized by T7 RNA polymerase. Mol Microbiol 42, 767-776.

Mock, T., and Thomas, D.N. (2005). Recent advances in sea-ice microbiology. Environ Microbiol 7, 605-619.

Molineux, I.J. (1991). Host-parasite interactions: recent developments in the genetics of abortive phage infections. New Biol 3, 230-236.

Netzband, R., and Pager, C.T. (2020). Epitranscriptomic marks: Emerging modulators of RNA virus gene expression. Wiley Interdiscip Rev RNA 11(3), e1576.

Oerum, S., Dégut, C., Barraud, P., and Tisné, C. (2017). m1A Post-Transcriptional Modification in tRNAs. Biomolecules 7, 20.

Osterhout, R.E., Figueroa, I.A., Keasling, J.D., and Arkin, A.P. (2007). Global analysis of host response to induction of a latent bacteriophage. BMC Microbiol 7, 82.

Pereira, M., Ribeiro, D.R., Pinheiro, M.M., Ferreira, M., Kellner, S., and Soares, A.R. (2021). m5U54 tRNA Hypomodification by Lack of TRMT2A Drives the Generation of tRNA-Derived Small RNAs. Int J Mol Sci 22, 2941.

Pluskal, T., Castillo, S., Villar-Briones, A., & Oresic, M. (2010). MZmine 2: modular framework for processing, visualizing, and analyzing mass spectrometry-based molecular profile data. BMC bioinformatics, 11, 395.

Qasim, M.S., Lampi, M., Garrido-Zabala, B., Bamford, D., Käkelä, R., Roine, E., Sarin, L.P. (2021) Shewanella glacialimarina nov. is a cold-adapted bacteria isolated from Baltic sea ice featuring putative sialic acid metabolism. Front Microbiol. Submitted.

Ranjan, N., and Rodnina, M.V. (2016). tRNA wobble modifications and protein homeostasis. Translation. Austin. 4(1), e1143076.

Rohrmann, G. F. (2019). Baculovirus Molecular Biology. (4th Ed.). National Center for Biotechnology Information (US). Ch 4.

Roundtree, I.A., Evans, M.E., Pan, T., and He, C. (2017). Dynamic RNA Modifications in Gene Expression Regulation. Cell 169, 1187-1200.

Rozov, A., Demeshkina, N., Khusainov, I., Westhof, E., Yusupov, M., and Yusupova, G. (2016). Novel base-pairing interactions at the tRNA wobble position crucial for accurate reading of the genetic code. Nat Commun 7, 10457.

Samson, J.E., Magadán, A.H., Sabri, M., and Moineau, S. (2013). Revenge of the phages: defeating bacterial defences. Nat Rev Microbiol 11, 675-687.

Schaefer, M., Kapoor, U., and Jantsch, M.F. (2017). Understanding RNA modifications: the promises and technological bottlenecks of the 'epitranscriptome'. Open Biol 7, 170077.

Senčilo, A., Luhtanen, A., Saarijärvi, M., Bamford, D.H., and Roine, E. (2015). Cold-active bacteriophages from the Baltic Sea ice have diverse genomes and virus-host interactions. Environ Microbiol 17, 3628-3641.

Suttle, C.A. (2007). Marine viruses — major players in the global ecosystem. Nat Rev Microbiol 5, 801-812.

Suzuki, T. (2021). The expanding world of tRNA modifications and their disease relevance. Nat Rev Mol Cell Biol 22, 375-392.

Vasu, K., and Nagaraja, V. (2013). Diverse Functions of Restriction-Modification Systems in Addition to Cellular Defense. Microbiol Mol Biol Rev 77, 53-72.

Vendeix, F.A.P., Dziergowska, A., Gustilo, E.M., Graham, W.D., Sproat, B., Malkiewicz, A., and Agris, P.F. (2008). Anticodon Domain Modifications Contribute Order to tRNA for Ribosome-Mediated Codon Binding. Biochemistry 47, 6117-6129.

Vogel, B.F., Venkateswaran, K., Satomi, M., and Gram, L. (2005). Identification of Shewanella baltica as the Most Important H2S-Producing Species during Iced Storage of Danish Marine Fish. Appl Environ Microbiol 71, 6689-6697.

Walsh, D., Mathews, M.B., and Mohr, I. (2013). Tinkering with Translation: Protein Synthesis in Virus-Infected Cells. Cold Spring Harb Perspect Biol 5, a012351.

Wang, Y., and Zhang, X. (2010). Genome Analysis of Deep-Sea Thermophilic Phage D6E. Appl Environ Microbiol 76, 7861-7866.

Wei, D., and Zhang, X. (2010). Proteomic Analysis of Interactions between a Deep-Sea Thermophilic Bacteriophage and Its Host at High Temperature. J Virol 84, 2365-2373.

Weitz, J.S., and Wilhelm, S.W. (2012). Ocean viruses and their effects on microbial communities and biogeochemical cycles. F1000 Biol Rep 4, 17.

Wilhelm, S.W., and Suttle, C.A. (1999). Viruses and Nutrient Cycles in the Sea: Viruses play critical roles in the structure and function of aquatic food webs. Bioscience 49, 781-788.

Zheng, C., Black, K.A., and Dos Santos, P.C. (2017). Diverse Mechanisms of Sulfur Decoration in Bacterial tRNA and Their Cellular Functions. Biomolecules 7(1), 33.

9 Supplementary Data

9.1 Figures & Tables

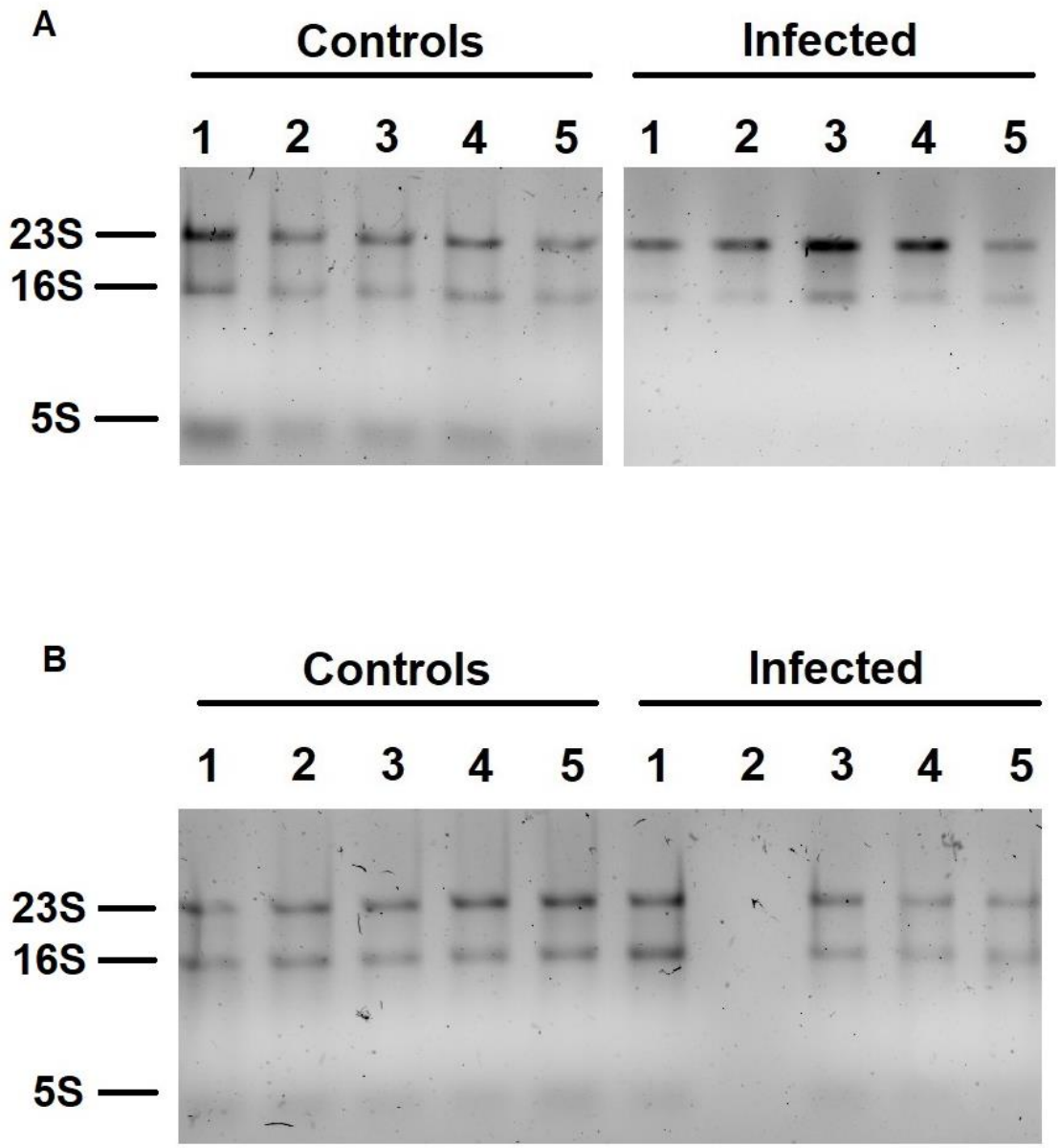

Supplemental Figure 1: SDS-PAGE of total-RNA for replicates 2 (A) and 3 (B). Ribosomal RNA bands marked on the left. Bands not visible for infected sample nr. 2 in the last replicate (B). As the quality and concentration of all total-RNA was shown to be acceptable, this gel was not redone.

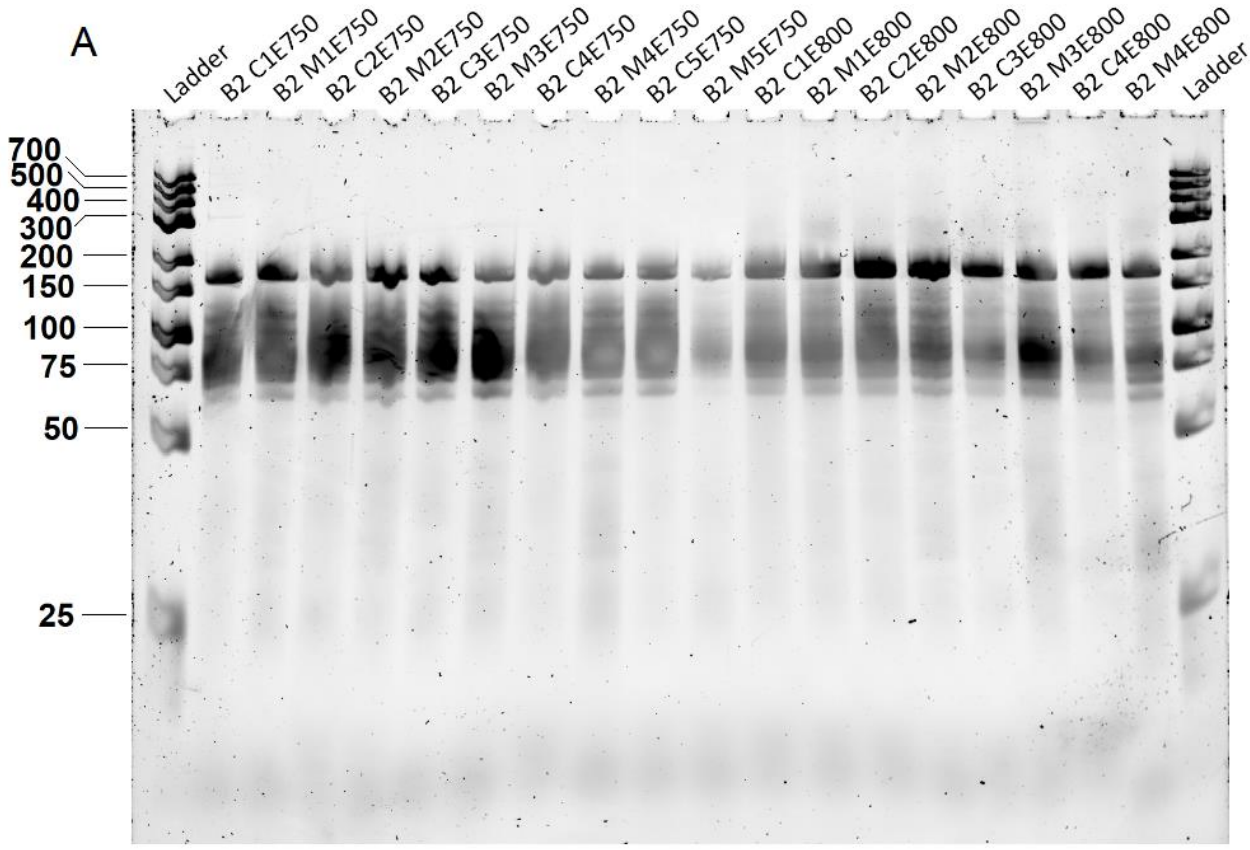
A
Ladder
B2 C1E750
B2 M1E750
B2 C2E750
B2 M2E750
B2 C3E750
B2 M3E750
B2 C4E750
B2 M4E750
B2 C5E750
B2 M5E750
B2 C1E800
B2 M1E800
B2 C2E800
B2 M2E800
B2 C3E800
B2 M3E800
B2 C4E800
B2 M4E800
Ladder
700
500
400
300
200
150
100
75
50
25

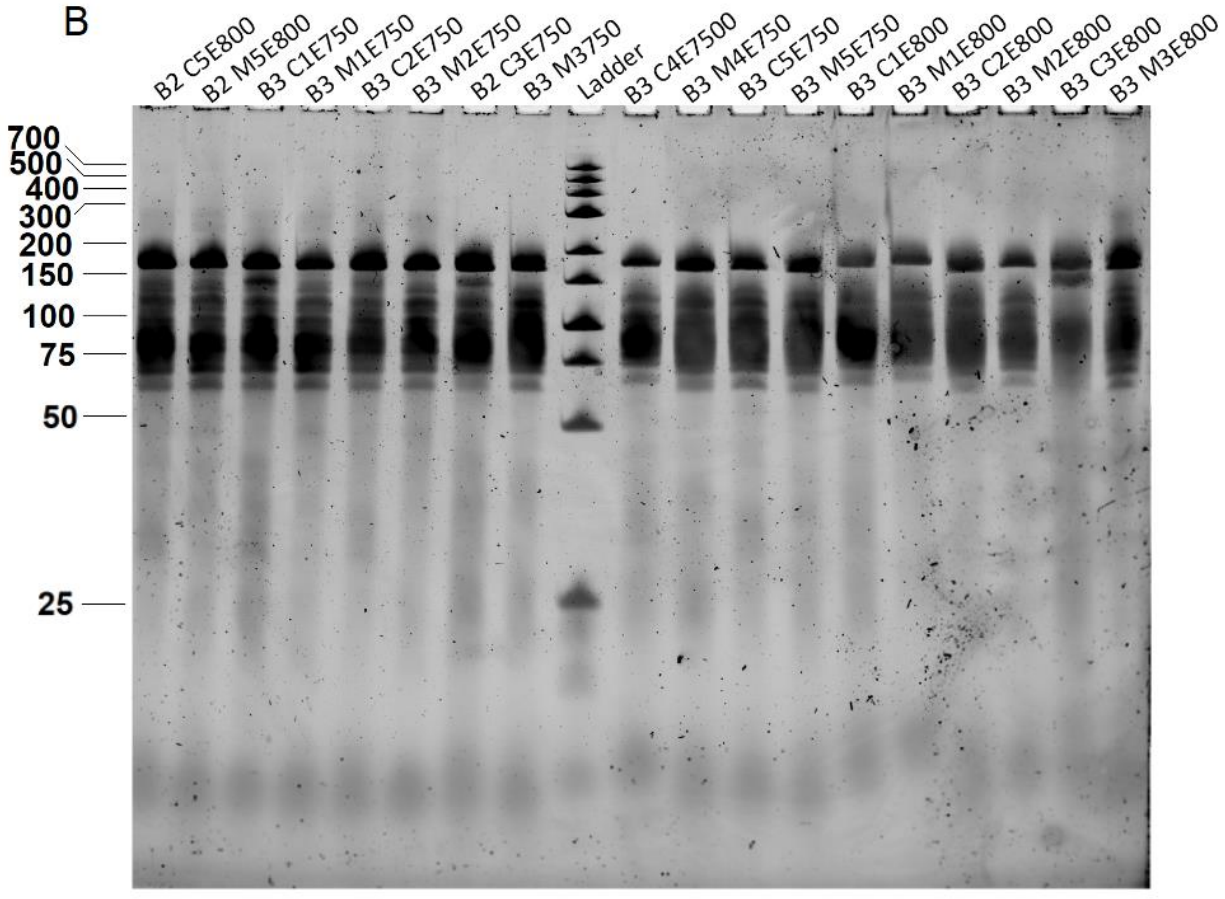
B
B2 C5E800
B2 M5E800
B3 C1E750
B3 M1E750
B3 C2E750
B3 M2E750
B2 C3E750
B3 M3750
Ladder
B3 C4E7500
B3 M4E750
B3 C5E750
B3 M5E750
B3 C1E800
B3 M1E800
B3 C2E800
B3 M2E800
B3 C3E800
B3 M3E800
700
500
400
300
200
150
100
75
50
25

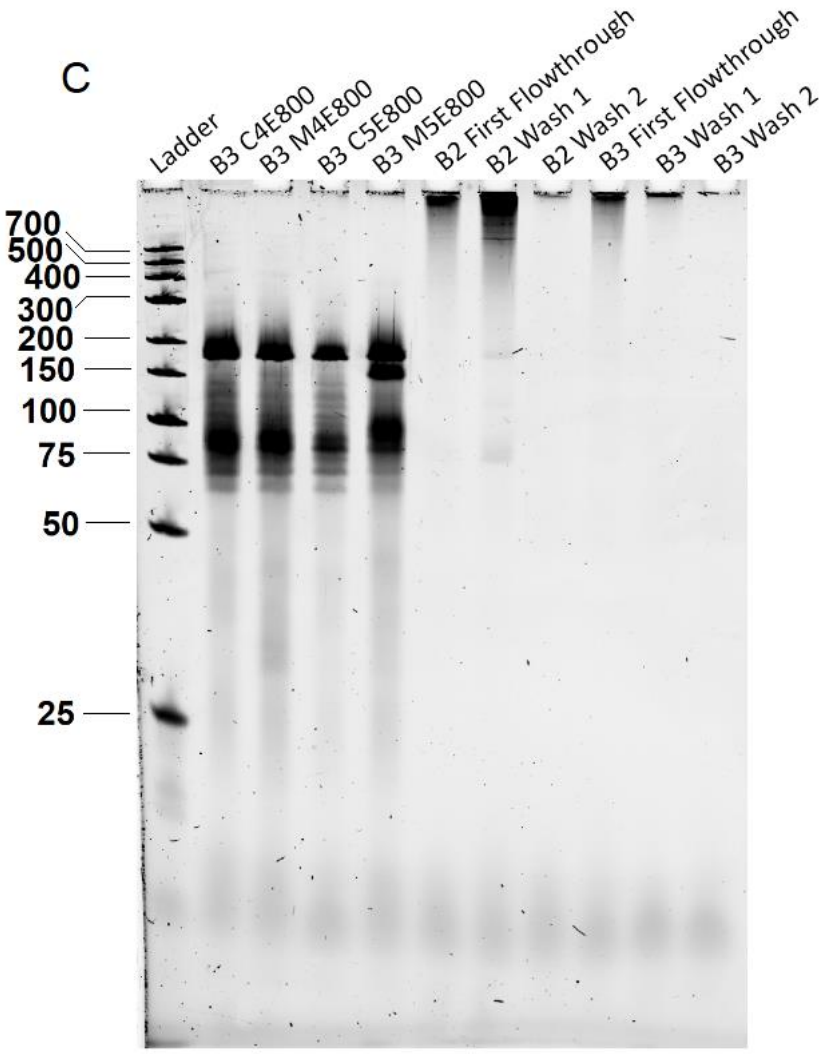

Supplemental Figure 2: Transfer-RNA seen on PAA-u gels for replicates 2 and 3, in addition to the controls of replicate 1. For replicate 2 and 3, the washes and first flowthrough from tRNA isolation was also investigated to observe possible leakage of RNA through the columns. Wells marked as B2/B3 for batch 2/3, C# and M# for controls and infected samples, and E750 and E800 for KCl concentrations of 750 mM and 800 mM in elution buffer.

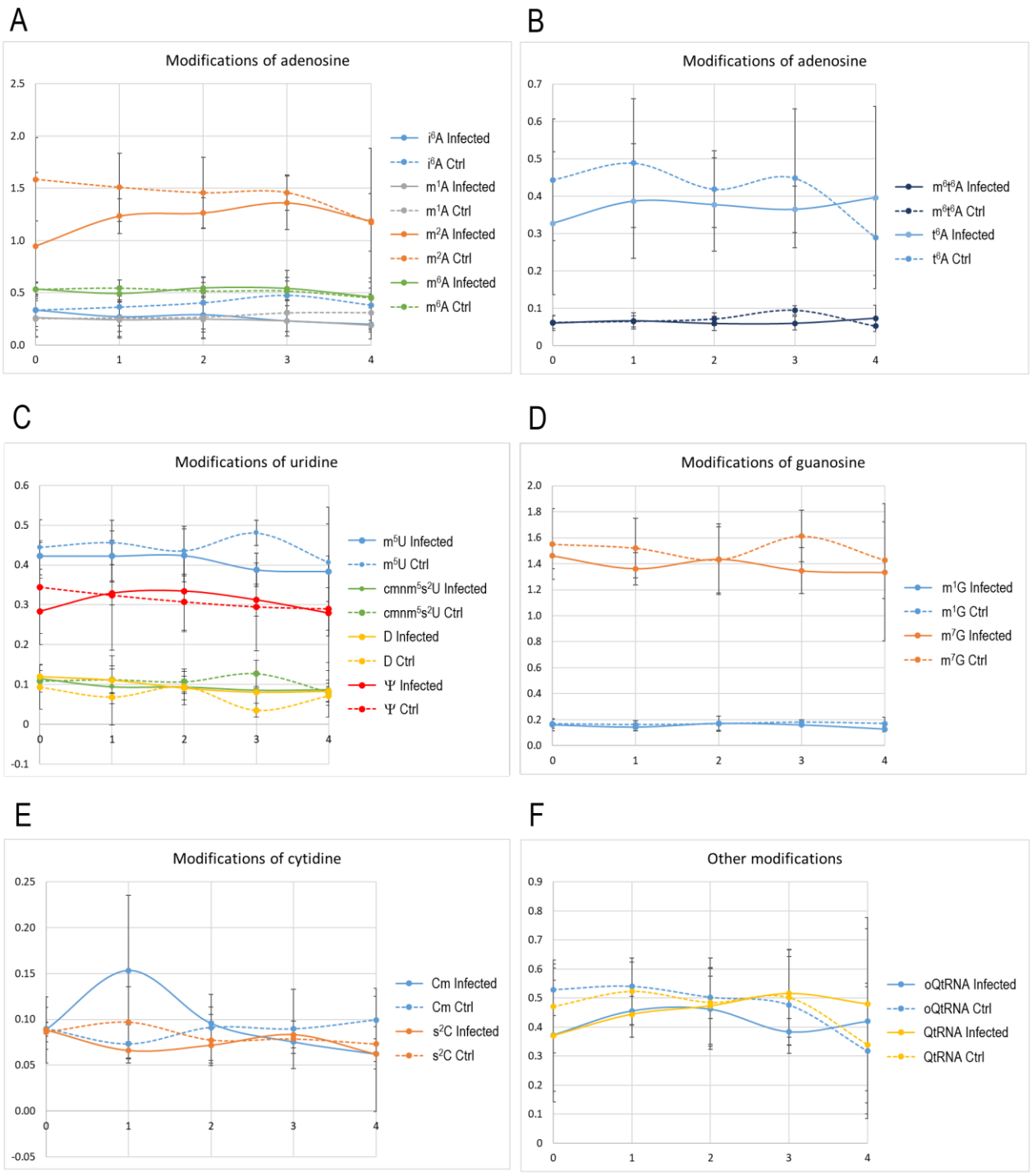

Supplemental Figure 3: All modifications found by UPLC-MS. Modifications for (A & B) adenosine, (C) uridine, (D) guanosine and (E) cytidine, as well as (F) other modifications included in graphs showing intensities. Y-axis represents the relative intensities normalized to the non-natural nucleoside $m^{1,3}\Psi$. X-axis numbered 0-4 represents the investigated time points of 0=0 min, 1=15 min, 2=30 min, 3=60 min, and 4=120 min. Error bars represent standard deviation of three replicates.

9.2 Recipes

Growth media

A

Rich 25% Marine broth	
Component	**For 1 l (g)**
Marine broth	9.35
Peptone	7.5
Yeast extract	1.5

B

Rich 25% Marine broth agar	
Component	**For 1 l (g)**
Marine broth	9.35
Peptone	7.5
Agar	15
Yeast extract	1.5

Supplemental Recipes 1: Growth media used for growing strain 4 cultures. (A) Liquid rMB used for all inoculations into liquid cultures. (B) Agar version of rMB was used for plating of cultures to calculate viable counts and plaque assays.

Gels & gel buffers

A

5x TBE buffer		
Component	**Final conc. (in 5x)**	**For 1 l**
Tris base	450 mM	54 g
Boric acid	450 mM	27.5 g
EDTA (0.5 M; pH 8.0)	10 mM	20 ml

B

Buffer A for polyacrylamide-urea gels (0% acrylamide)						
Component	**Stock conc.**	**Final conc.**	**For 100 ml**	**For 200 ml**	**For 400 ml**	**For 500 ml**
Urea	-	7 M	42.04 g	84.08 g	168.16 g	210.21 g
TBE	5x	0.5x	10 ml	20 ml	40 ml	50 ml

C

Buffer B for polyacrylamide-urea gels (20% acrylamide)						
Component	**Stock conc.**	**Final conc.**	**For 100 ml**	**For 200 ml**	**For 400 ml**	**For 500 ml**
Urea	-	7 M	42.04 g	84.08 g	168.16 g	210.21 g
TBE	5x	0.5x	10 ml	20 ml	40 ml	50 ml
Acrylamide (19:1)	40%	20%	50 ml	100 ml	200 ml	250 ml

D

PAA gels (20 ml per gel)						
	8% gels			**10% gels**		
	20 ml (1 gel)	**40 ml (2 gels)**	**60 ml (3 gels)**	**20 ml (1 gel)**	**40 ml (2 gels)**	**60 ml (3 gels)**
Buffer A	12 ml	24 ml	36 ml	10 ml	20 ml	30 ml
Buffer B	8 ml	16 ml	24 ml	10 ml	20 ml	30 ml
TEMED	20 µl	40 µl	60 µl	20 µl	40 µl	60 µl
10% APS	200 µl	400 µl	600 µl	200 µl	400 µl	600 µl

Supplemental Recipes 2: Recipes for (A) TBE buffer to use as running buffer, (B) buffer A part of the PAA-U gels, (C) buffer B part of the PAA-U gels, and (D) PAA-U gels for confirming the quality of tRNA.

Loading buffers & staining

A

6x DNA loading buffer			
Component	**For 10 ml**	**For 20 ml**	**For 40 ml**
1 M Tris-HCl, pH 7.6	100 µl	200 µl	400 µl
bromophenol blue	3 mg	6 mg	12 mg
xylene cyanol FF	3 mg	6 mg	12 mg
Orange G	10 mg	20 mg	40 mg
80% glycerol	7.5 ml	15 ml	30 ml
0.5 M EDTA	1.2 ml	2.4 ml	4.8 ml

B

2x RNA loading buffer			
Component	**For 10 ml**	**For 20 ml**	**For 40 ml**
Formamide (pure)	9 ml	18 ml	36 ml
5x TBE	1 ml	2 ml	4 ml
20% SDS	25 µl	50 µl	100 µl
bromophenol blue	2.5 mg	5 mg	10 mg
xylene cyanol FF	1 mg	2 mg	4 mg

C

1.5x RNA loading buffer			
Component	**For 10 ml**	**For 20 ml**	**For 40 ml**
Formamide (pure)	9 ml	18 ml	36 ml
10x TBE	1 ml	2 ml	4 ml
Orange G	7.5 mg	15 mg	30 mg

D

Coomassie for gel staining	
Component	**For 1 ml**
alpha-Cyclodextrin	20 g
2-Hydroxyethylcellulose	3 g
85% Orthophosphoric acid	50 ml
99.6% Ethanol	20 ml
Coomassie G250	45 mg

Supplemental Recipes 3: Recipes for (A) DNA loading buffer for viral protein visualization, (B) RNA buffer for total-RNA gels, (C) RNA buffer for tRNA gels, and (D) Coomassie stain for protein staining.

RNA-isolation

A

Homemade Trizol for RNA-isolation		
Component	**Final conc.**	**For 100 ml**
Phenol, Saturated (pH 4.3, Liquid)	38%	38 ml
Guanidine thiocyanate	0.8 M	11.82 g
Ammonium thiocyanate	0.4 M	7.61 g
Sodium acetate (pH 5.0, 3M solution)	0.1 M	3.33 ml
Glycerol	5%	5 ml
MQ H_2O	-	To 100 ml

B

		Equilibration buffer		Wash buffer		Elution buffer	
Component	**Stock conc.**	**Final conc.**	**For 350 ml (ml)**	**Final conc.**	**For 1 l (ml)**	**Final conc.**	**For 350 ml (ml)**
Tris (pH 6.3)	1 M	10 mM	3.5	10 mM	10	10 mM	3.5
EtOH	99.6%	15%	52.5	15%	150	15%	52.5
KCl	3 M	200 mM	23.3	300 mM	100	750 mM	87.5
TX-100	10%	0.15%	5.25	-	-	-	-
MQ H_2O	-	-	265.45	-	740	-	236

C

Enzyme master mix (tRNA digestion)		
Component	**Stock conc.**	**For each sample**
NaOAc (pH 5.5)	200 mM	3.0 µl
Nuclease P1	10x	3.2 µl
Fast Alkaline Phosphatase	10x	2.0 µl
50 mM $ZnCl_2$	50 mM	2.0 µl

Supplemental Recipes 4: Recipes used for RNA-isolation including (A) homemade Trizol, (B) buffers for tRNA isolation using AX-100 columns, and (C) the master mix used for digestion of tRNA for UPLC-MS.